Spring 2015

Investigating the binding potential and downstream effects of ferrocene/ ruthenium (III) complexes with RNA

Mildred Apollo Kissai
Bard College

Investigating the binding potential and downstream effects of ferrocene/ruthenium(III) complexes with RNA

Senior Project Submitted to
The Division of Science, Math and Computing
of Bard College

by
Mildred Apollo Kissai

Annandale-on-Hudson, New York
May 2015

Table of Contents

Abstract

Cisplatin, one of the most popular chemotherapeutic drugs on the market today, battles cancer by binding to DNA, and causing kinks which obstruct DNA replication and transcription. As a result, cisplatin halts cell proliferation of not only fast-dividing cancerous cells but healthy cells as well. To circumvent the shortcomings of cisplatin, the Anderson lab has synthesized a class of ruthenium (III)/ ferrocene compounds, named the RuLX series. These new hetero-multinuclear complexes may have greater selectivity between cancerous and healthy cells through a proposed synergistic mechanism of their metal centers. Previous work on these novel complexes has demonstrated that they interact with DNA and proteins, suggesting that they may share similar molecular targets as cisplatin. RNA has merged as a new molecular target for metal therapeutics not only due to its chemical similarity with DNA, but also due to its essential role in cellular function. Many metallochemotheraputics target RNA as well as other biomolecules in their mode of action.

The *in vitro* binding affinity of the RuLX complexes with RNA was investigated using a 504-base RNA encoding the dihydrofolate reductase enzyme. Evidence suggests that RuL2 and RuL3 have a stronger binding affinity to RNA than RuL1. Moreover, *in vitro* translation of the DHFR mRNA was carried out to observe the potential downstream effects of these interactions. All three complexes exhibited a dose-dependent reduction of DHFR enzyme activity. Investigations with RuL2 specifically, suggest that its inhibition of DHFR activity is likely due to the metal complex binding to RNA. Explorative controls show that RuL2 does not significantly inhibit enzyme activity or ribosomal protein activity.

Dedication

For my parents – Apollo Giese Kissai and Nurru Lameck Mligiliche, it is because of your sacrifices and unconditional support for me that this work was made possible

Acknowledgements

I would like to thank my family, for their unwavering faith and support all my life. Mama, Baba, Pendo and Ka'grey you've kept me going through out my college years. All I have and will accomplish is, no doubt, in debt to all of you. My family away from home, Hamadi Mkambavange, Elizabeth Mkambavange, and the precious Noah and Amani Mkambavange, thank you for making me feel at home during the holidays and providing me a safe haven during my undergraduate years. I love you all.

I cannot continue without thanking my advisor Swapan Jain for his support, patience, guidance, and especially, for his confidence in me throughout my undergraduate career. I would also like to thank Brooke Jude for her support while I was trying to manage both the biology and chemistry majors. I would also like to thank the Anderson lab, especially Kody Chen and Sumedha Guha for having prepared the complexes that I used for my senior project. Moreover, thank you for being wonderful sources of support and help during the project process. I huge thank you to Nushrat Hoque, for being a great mentor, a great friend and being the voice of reason during my many times of crisis. Thank you for the texts of encouragement throughout my writing process.

I also want to give my dear roomies a shout out. The caring soul that is Alexandra Smith and the fabulous existence that is Gouled Ahmed, living with you for the past year has given me some of my cherished moments of my college career.

To all my friends, your friendships make my life a wonderful experience. I look forward to sharing our next great adventure.

List of Tables and Figures

1. Introduction

1.1 Cancer

Cancer, one of the leading causes of death worldwide, is characterized by uncontrolled cellular proliferation and avoidance of programmed cell death, or apoptosis[1]. According to Hanahan and Weinberg, cancer can be categorized by monitoring the hallmark differences that cancerous cells develop in comparison to healthy cells. Cancerous cells develop an extensive list of capabilities that enable their survival and proliferation throughout an organism. These acquired capabilities include the ability to be self-sufficient in the production and utilization of growth signals, an insensitivity to antigrowth signals, a cunning evasion of apoptosis, an almost limitless replicative potential, a sustained ability to form new blood vessels from old ones (angiogenesis), an ability to invade new tissues, and metastasis[2]. Cancer malignancy begins when cancerous cells gain the potential to metastasize, spreading to distant areas of the body through the circulatory and lymphatic system[2]. Cancerous cell's ability to invade surrounding tissue, colonize, and destroy other tissues throughout the body has been tied to their cellular motility[3]. Due to robust research in the field, additional enabling traits that help cancer cells survive have been stipulated. These traits include the reprogramming of energy harvesting mechanisms to require low oxygen intake, the ability of cancerous cells to evade destruction from the immune system, and the development of tumor-promoting inflammation[4]. The discoveries of these additional mechanisms that aid in cancer malignancy have been the focus of current anti-cancer therapeutic research.

Cancer arises as a result of somatic mutations in which genes that become mutationally under-expressed or abnormally overexpressed contribute to tumor formation, and are called protoconcogenes[5]. Moreover, healthy cells can become cancerous through spontaneous or

inherited mutations in tumor suppressor genes, which are genetic suppressors of tumor growth, mutations in oncogenes, which are genes that have the potential to promote cancerous growth, or other somatic mutations that give rise to oncogenes[5].

Cancers come in diverse physiological and chemical make-up. Fittingly, different modes of treating the disease have been developed. Some of the commonly used treatments in human cancers include: surgery, radiation therapy, immunotherapy, stem cell transplants and chemotherapy[6]. First, surgery combats cancer by excising the malignancy out of the body; it is particularly good at combating benign (non-metastasized) cancerous growth[6]. Second, radiation therapy uses high-energy radiation to target and destroy cancer cells[6]. Radiation therapy is one of the most common methods of cancer treatment out there today[6]. Third, immunotherapy, one of the lesser common cancer treatment methods, involves stimulating the immune system to work more efficiently in destroying cancer cells[6]. It may also involve supplying the immune system with synthesized proteins to stimulate anticancer activity[6]. Fourth, stem cell transplants entail a full transplantation of a person's peripheral blood, bone marrow, and cord blood[6]. This treatment is particularly useful in combating cancers that affect the circulatory and lymphatic system[6].

Finally, the most widely known treatment method for cancer, chemotherapy, involves the administration of combinatorial drugs, usually intravenously, to combat the growth and spread of cancer cells[6]. Targeted therapy, which involves the use of chemicals more specifically tailored for cancerous cells in order to lessen the collateral destruction of healthy cells, is also an option for persons affected with cancer[6]. All of the aforementioned treatments are often used synergistically with each other, depending on the particular cancer type, to effectively destroy the cancerous cells.

1.2 Chemotherapy complex: Cisplatin

1.2.1 Discovery of cisplatin

Cis-diaminedichloroplatinum(II), or cisplatin is a platinum based compound commonly used as a chemotherapy drug. It was discovered by, Barnett Rosenberg, a biophysicist at the University of Michigan, who at the time, was examining the impact of electrical current in cell division of *Escherichia coli* (*E. coli)*[7,8]. Unexpectedly, Rosenberg et al. found that interaction of the platinum electrodes and the ammonium chloride buffer caused filamentous growth and the inhibition of cell division in *E. coli*[7,8]. Since the platinum species proved to be potent in inhibiting bacterial cell division, it was reasoned that the platinum species might offer similar antiproliferation mechanisms when tested on rapidly dividing cancerous cells. In order to test the anticancer potential of their platinum species, Rosenberg et al. tested cisplatin, and ten other group 10 transition metal complexes, on small solid sarcoma 180 tumors in mice[8,9]. They found that cisplatin, and some analogs, completely inhibited the development of tumor growth if administered one day after tumor inoculation in mice. It also yielded impressive results when it was tested on different cancer types using different animal models[9]. Cisplatin's effectiveness in combatting cancer led the FDA to approve it for clinical applications in 1978[10]. Cisplatin is so potent in combatting cancer that it still boasts a greater than ninety percent cure rate for promptly diagnosed testicular cancer[10].

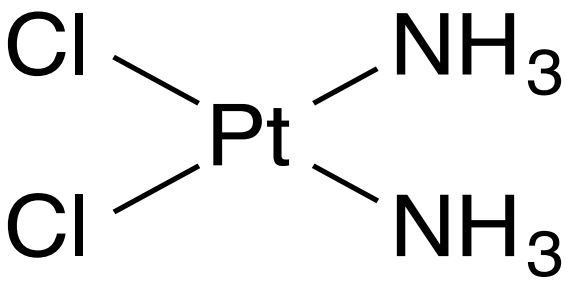

Figure 1: The chemical structure of cisplatin.

1.2.2 Cisplatin's mechanism of action

Much of cisplatin's possible mechanisms of action have been elucidated after its clinical approval due to the emergence of metallochemotherapeutic research. Cisplatin primarily enters the cell through passive diffusion and active transport mediated by the transporter protein Ctr1p[10,13]. The low intracellular chlorine ion concentration of the physiological environment facilitates the hydrolysis and activation of the cisplatin complex into its aquatic form, $[Pt(NH_3)_2Cl(OH)_2]^+$ and $[Pt(NH_3)_2(OH_2)2]^{2+}$ [10]. In its active form, cisplatin can react easily with cellular components such as DNA, RNA, proteins and membrane phospholipids[13]. Although cisplatin can react with many cellular components, DNA is believed to be its primary target. Cisplatin binds to DNA by forming inter-strand and intra-strand adducts with the N^7 atom of purine bases[11].

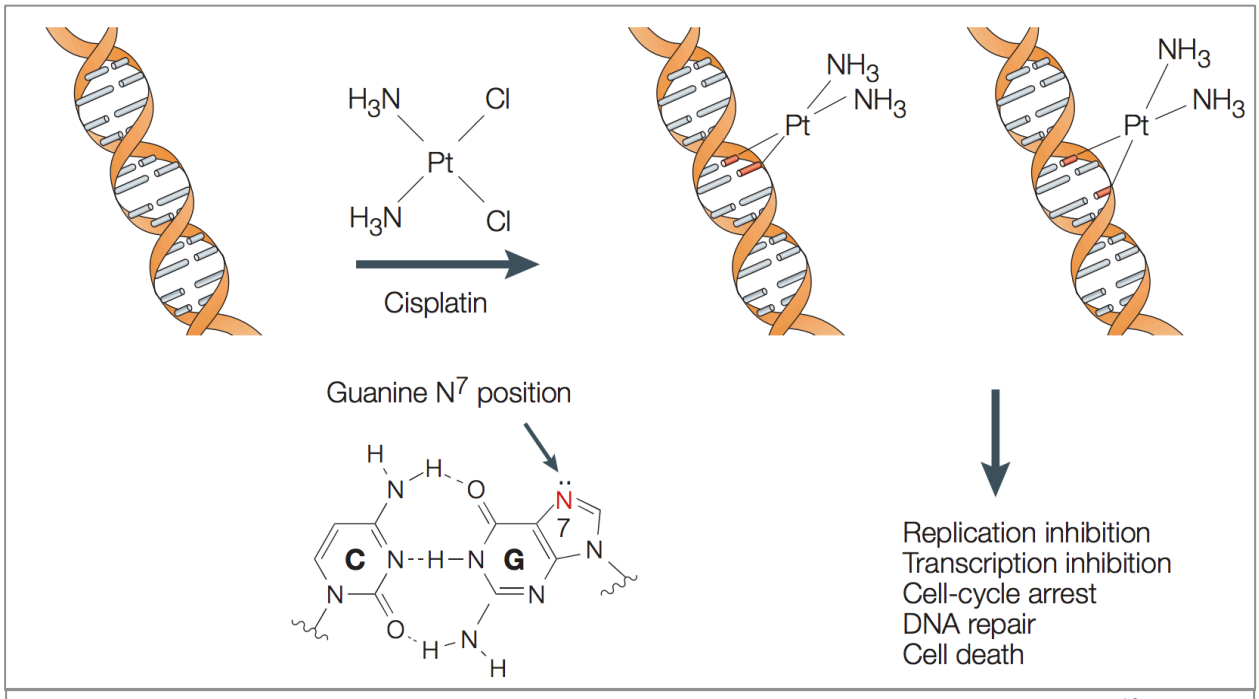

Figure 2: Mechanism of action of cisplatin anti-cancer activity by binding with DNA[12]

In the aquated form of cisplatin, the weakly bound hydroxide ligand is easily displaced, allowing the platinum center to coordinate to the N^7 nitrogen of the purine bases and form

covalent bonds[11]. This results in primarily 1,2 or 1,3-intrastrand crosslinks and a lower number of inter-strand crosslinks[11]. The major adducts formed from cisplatin binding are GpG (40-50%) and ApG (23-38%) intrastrand crosslinks as well as interstrand crosslinks accounting for 1-7% of adduct formation[14]. The N^7 nitrogen is the most accessible atom for cisplatin coordination because it is not only located in the major groove of the DNA helix, but it also possesses a lone pair available for coordination. Once bonded, cisplatin causes a major structural distortion of the DNA double helix, disrupts base pairing, and widens the minor groove. Cisplatin binding produces a rigid bend in DNA of 30-35° directed toward the major groove and a localized unwinding of the DNA helix of 13° [14]. As a result, essential biological functions including DNA repair, replication and transcription are inhibited[15]. The Pt-DNA adducts additionally activate several signal transduction pathways including ART, p53, p73 and MAPK which consequently activate apoptosis[15]. Sometimes, cisplatin damaged DNA elicits cellular repair mechanisms. If these repairs are unsuccessful, apoptosis is activated to terminate the cell. Cisplatin has also been shown to hinder mRNA from directing *in vitro* peptide synthesis by preventing the formation of the complete translation initiation complex[16, 17]. Nevertheless, it is cisplatin's binding to DNA that is credited as the mode of action due to which the proliferation of cells is inhibited.

1.2.3 Cisplatin's shortcomings

Although cisplatin can boast great clinical success, it does come with some potent drawbacks. One of which is the unselective cytotoxicity that cisplatin bears to both healthy and cancerous cells which causes severe side effects[10]. These include damage to nearby convoluted tubes of the kidney, extreme nausea and intense vomiting[9]. Moreover, although it was expected for some tissues to bear spontaneous resistance to cisplatin, recent research has revealed that

tissues can develop cisplatin resistance over time. The mechanisms by which cells resist cisplatin-induced cytotoxicity include reduced cellular uptake of cisplatin, the ability to chemically inactivate the compound and DNA adduct repair[18]. Reduced cisplatin accumulation in resistant cells is due to an inhibition in cellular uptake or an increase in drug efflux, or both[18]. The inactivation of cisplatin has been attributed to the non-enzymatic and rate-limiting interactions between aquated cisplatin and endogenous nucleophiles such as glutathione, methionine, metallothionein and several proteins[18]. DNA adduct repair via the nucleotide excision repair mechanism reduces the number of Pt-DNA adducts and as a result, reduces the cascading of the apoptotic signal[18]. Furthermore, cisplatin is not active against all primary tumors. Notable exceptions include breast cancer, prostate cancer and colorectal cancers[20]. It is also minimally effective in combatting metastatic cancer due to its mostly cytotoxic mechanism of action[20]. As cancers become more resistant to common chemotherapeutic drugs like cisplatin, and other platinum centered drugs, a focus in biomedical research has centered on developing new organometallic complexes to circumvent the shortcomings of cisplatin.

1.3 Ruthenium complexes

1.3.1 Prodrug selectivity

In organometallic research, ruthenium complexes have gained popularity as potential chemotherapeutics due to their unique reactivity. Ruthenium (III) complexes modeled after cisplatin have demonstrated antitumor properties and lower cytotoxicity than cisplatin. The octahedral geometry of ruthenium (II) and (III) complexes, as opposed to the square planar geometry of cisplatin, lends evidence to the hypothesis that ruthenium complexes function differently from platinum complexes[21]. For instance, while adjacent intra-strand G-G crosslinks with *cis*-Ruthenium ions are possible, they are sterically more hindered due to its octahedral

geometry[21]. Moreover, research suggests that Ru (III) complexes function as a prodrug and work by 'activation by reduction' mechanism. Ru (III) complexes are activated by their *in vivo* reduction into the chemically active Ru (II) in order to more effectively coordinate to biomolecules[21]. The lower charge and the reduced π-bonding effects of Ru (II) that make Ru (II) more reactive than Ru(III) [21]. Moreover, the hypoxic and acidic microenvironment of tumor cells caused by excess lactic acid creates a low electrochemical potential inside the cell that allows for Ru(III) to be reduced to Ru(II) selectively in tumor tissue[21]. Lactic acid accumulation comes about due to low intracellular oxygen content, which is caused by the lag between the rate of angiogenesis and the rate of cell growth and division[2]. As the rate of cancerous cell division increases, this causes a build-up of tumor tissue that is ineffectively vascularized and as a result, hypoxic. Until the rate of angiogenesis catches up to the rate of cancerous cell growth and division, the tumor tissue microenvironment remains hypoxic[13]. Hence, the higher Ru(II) compared to Ru(III) concentration in cancerous cells coupled with the inherently higher reactivity of Ru(II) is thought to make ruthenium based prodrugs somewhat more selective towards cancerous cells.

1.3.2 New Anti-tumor Metastasis Inhibitor (NAMI) and its analog NAMI-A

Early ruthenium anticancer compounds, which included: *cis*- and *trans*-[RuCl(DMSO)] complexes, paved the way for the design of current clinically used ruthenium based prodrugs like Na{trans-[Cl_4(DMSO)(Im)Ru]}, known as NAMI and its analog, Na{trans-Cl_4(DMSO)(Im)Ru]}, also known as NAMI-A[22]. Because these ruthenium complexes can lose both their chloride and DMSO ligands, the mode with which they bind to biomolecules is more flexible than cisplatin[23]. Heterocyclic additions, such as imidazole and indazole, to ruthenium-

based drugs have also shown to have positive impacts on their anti-proliferation properties[19]. NAMI is active against a broad range of tumors including Lewis lung carcinoma, B16 melanoma, and MCa mammary carcinoma[23]. Notably, research has found that only a very low fraction of the NAMI reaches the tumor target[23]. In addition, its activity appears to be independent of its concentration in tumor cells, and its major mechanism of action does not involve DNA binding[23].

Rather than cytotoxicity, NAMI combats cancer by increasing the resistance to the formation of tumor metastases. It accomplishes this without enhanced antigenicity or instigating immunological responses[23]. NAMI is also credited with down regulating type-IV collagenolytic activity and metastatic potential of MCa mammary carcinoma. NAMI significantly increases the mRNAs of MMP-2, a metalloproteinase capable of degrading the extracellular matrix, and TIMP-2, the specific tissue inhibitor of the aforementioned enzyme at dosages that prevent metastasis in lung cancer[23]. This causes a pronounced increase of extracellular matrix components in the tumor parenchyma and around tumor blood vessels; excess extracellular matrix components are thought to hinder both metastasis formation and blood flow to the tumor[23].

NAMI-A, a chemical analog of NAMI where the sodium counter-ion is replaced with an imidazolium ion, also boasts antimetastatic properties. *In vitro*, NAMI-A has comparable binding affinity to DNA as cisplatin[24]. However, *in vivo* studies using four different tumor cell lines revealed that NAMI-A has a much lower affinity

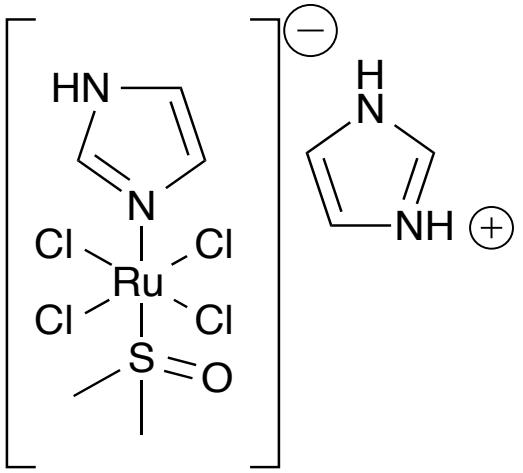

Figure 3:Chemical structure of NAMI-A

to DNA than cisplatin[24]. NAMI-A-induced DNA kinks were only detected at extremely high dosages compared to cisplatin. Moreover, the frequency of NAMI-A's Ru-GG and Ru-AG intrastrand adducts to DNA are meek compared to the more plentiful cisplatin intrastrand adducts[25]. It is unsurprising that the lower rate of NAMI-A's cellular cytotoxicity was attributed to its lower intrastrand adduct formation[24]. However, NAMI-A is capable not only of preventing the formation of tumor metastases but also, of inhibiting their growth in a similar fashion to NAMI.

1.4 Ferrocene complexes

Another class of metal complexes that have been shown to exhibit antineoplastic effects are iron-containing compounds. In particular, ferrocene−a compound containing two π-bonded cyclopentadienyl ligands on an iron molecule. This compound's medicinal properties were first investigated because it was the first iron-containing compound found to exhibit antiproliferative properties[27]. Ferrocene complexes differ from platinum or ruthenium complexes in three major ways. Firstly, the central iron atom exists in the oxidation state +2 in ferrocene and the oxidation state +3 in ferrocenium ions[28]. Secondly, they lack any *cis*-halide ligands able to be dissociated[24]. Thirdly, they contain two cyclopentadienyl rings in a sandwiched arrangement; the central iron is tightly bound and is unlikely participate in further coordination bonds[28].

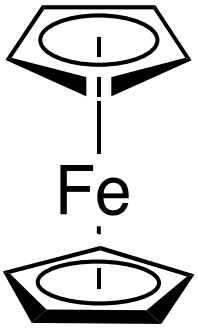

Figure 4: The chemical structure of ferroccene.

Moreover, ferrocene bears little cytotoxicity. In murine model experiments, it was shown that orally administered ferrocene is not only non-toxic, but it is degraded (enzymatically

hydroxylated) in the liver and excreted in urine[11]. Ferrocene can additionally undergo a one-electron oxidation to give the ferrocenium cation. This cation is easily soluble due to its salt-like qualities. It is also relatively stable and the redox reaction from which it was generated is also reversible[11]. The ferrocenium salt-like cations exhibited antineoplastic activity against Ehrlich ascites tumor (EAT) cell lines in CF1 mice, which are very resistant to classical antitumor agents such as platinum centered metal complexes[27]. While they found that the ferrocene complex itself bears no recognizable antitumor effects on these cells lines, they found that ferrocenium salt-like complexes boast incredible inhibitory effects, with some 100% cure rates of tumors[27]. Other ferrocene derivatives have shown significant anticancer potential, for instance that of tamoxifen and its derivatives. Tamoxifen is the front-line chemotherapeutic agent for patients with hormone-dependent breast cancer. Its active metabolite is hydrotamixifen. Tamoxifen combats breast cancer by competitively binding to the ERα subtype and repressing estradiol-mediated DNA transcription in the tumor tissue[11].

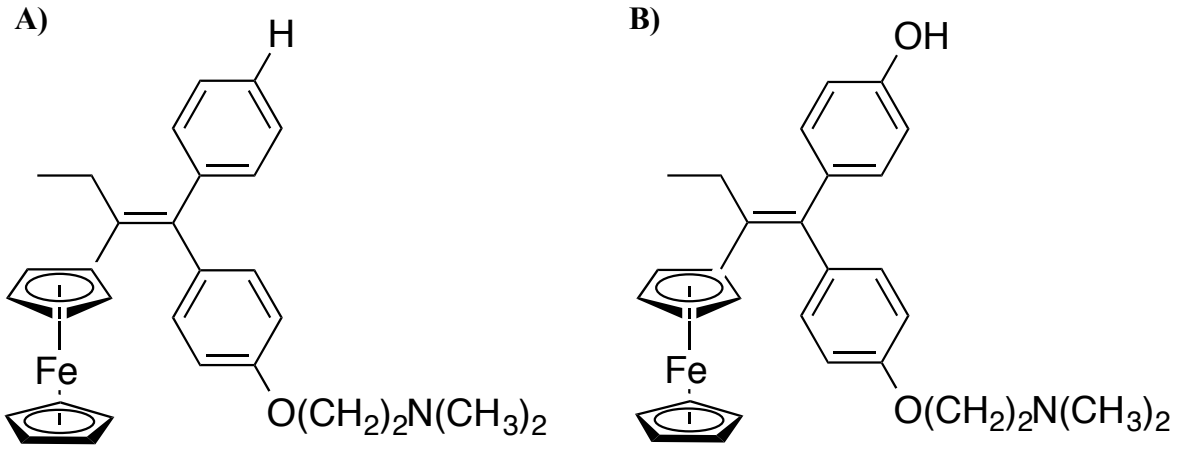

Figure 5: The chemical structure of **A)** Ferrotamoxifen and **B)** Ferro-hydrotamoxifen.[11]

Although the mechanism of action of these ferrocenium salts has yet to be elucidated, it is proposed that their cytotoxic activity is not based on their direct linking to DNA, but rather

on their ability to generate oxygen active species that induce oxidative DNA damage[24]. It is thought that ferrocenium cations generate hydroxyl radicals in physiological conditions that damage DNA via fenton-type reactions[28]. The tumor microenvironment, which contains increased concentrations of hydrogen peroxide, allows for the production of these radicals.

Un-substituted ferrocene is insoluble in water; it is unsurprising that it does not display any tumor inhibiting activity. However, once inserted into the target cells, it could interconvert to the ferrocenium cation, and vice versa, depending upon the redox potential of the tumor microenvironment[28]. Hence, much like the ruthenium containing complexes, ferrocenium salts have the potential to selective target cancerous cells while causing little harm to healthy cells.

1.5 Multinuclear compounds

To circumvent cellular resistance to cisplatin, multiplatinum complexes modeled after cisplatin were developed[14]. These complexes bound to DNA in a similar manner to cisplatin. However, due to their larger size and varied ligands, these multiplatinum complexes were able to form non-directional DNA adducts, to form a greater number of interstrand adducts compared to cisplatin, and to induce conformational type changes to both A- and Z-type DNA[14]. It has been suggested that DNA repair proteins weakly recognize DNA adducts resultant from multiplatinum complexes because of their different characteristics compared to cisplatin induced DNA adducts. Consequently, the structural changes caused by multiplatinum complexes bypass recognition from DNA repair proteins and more successfully, inhibit DNA transcription and replication[14].

Moreover, due to the discovered anticancer potential of different transition metal complexes, recent research has sought to combine different metal centers into one complex that would posses the best qualities of all its components. Some mixed-metal species that has afforded some success in heteromultinuclear antineoplastic research are a series of complexes

that couple a light absorbing ruthenium (II) or osmium (II) metal center to a reactive platinum site that contains the *cis*-dichloride platinum moiety. This moiety is through to be responsible for cisplatin's anticancer activity [29-31]. Brewer and colleagues found that their novel complexes awarded a higher percentage of interstrand crosslinks compared to cisplatin. Furthermore, tridentate bridged Ru(II)-Pt(II) and tetrametallic multinuclear complexes were also found to have more robust chemical interactions with DNA than cisplatin[29- 31]. Multinuclear complexes have the potential to exhibit synergistic effects that may result in a greater impact on their target biological system than their mononuclear counterparts[32]

Anderson et al. have developed several heteromultinuclear complexes containing both ruthenium and platinum centers that have demonstrated antineoplastic and anti-metastatic potential[32, 33]. Na_2 {trans, cis, trans- [Ru $^{(III)}Cl_4$(DMSO-S)(-μ-pyz)]$_2$Pt$^{(II)}Cl_2$}, otherwise known as AH197, a trinuclear complex with characteristics of both NAMI and cisplatin, was shown to bind DNA with better efficacy than cisplatin[33]. The complex also demonstrated greater inhibition of cell proliferation, using a *S. cervasie* model system, than both NAMI-A and cisplatin[32]. Moreover, AH197 appears to be more cytotoxic than cisplatin and KP1019−another ruthenium centered anticancer compound, in leukemia (CCRF-CEM), NSC lung, breast (BT-549), and colon (COLO 205) cancer cell lines[33]. Although its mechanism of action has not been elucidated, it appears that AH197 binds RNA and terminates primer

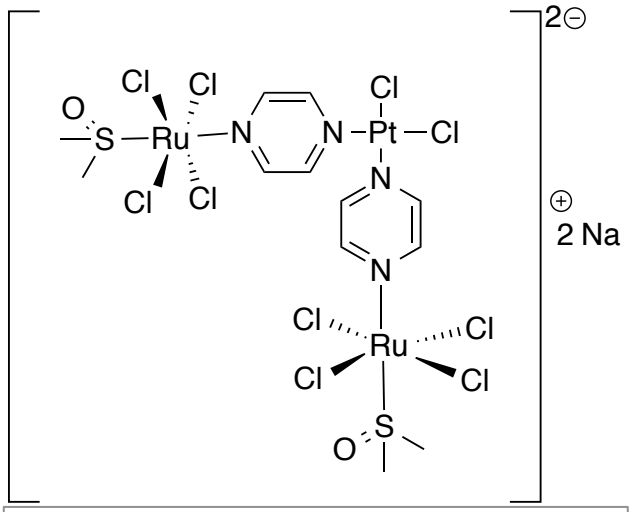

Figure 6: The chemical structure of AH197[25]

extension in *in vitro* reverse transcription assays by generally inhibiting DNA polymerization[34]. This suggests that AH197 targets nucleic acids much like cisplatin.

The Anderson lab also synthesized another compound, [K][$Ru^{III}Cl_4$ (DMSO)(-μ-pyz)-Pt^{II}(DMSO-S)Cl_2], also known as IT127, a dinuclear complex which showed similar anticancer potential[32]. IT127 also has the ability to inhibit cell motility at a degree comparable to NAMI-A[32]. Moreover, electrophoretic mobility shift assays demonstrated that IT127 has a higher binding affinity for plasmid DNA than both cisplatin and AH197[32]. This suggests that this hetero-multinuclear complex may target the nucleic acids, much like cisplatin, but it may inhibit metastasis in a similar manner to NAMI-A.

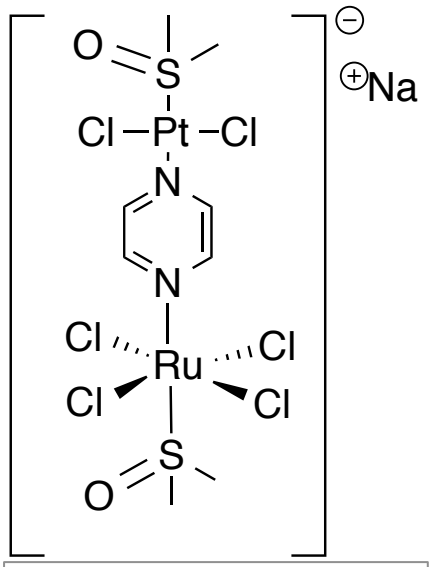

Figure 7: The chemical structure of IT127[25]

Recently, the Anderson lab developed a new class of compounds that combine the structure of NAMI-A with a ferrocene moiety in order to explore potential synergistic effects from the combination of two anti-proliferation compounds[35]. Hoping to combine their low cytotoxicity and potential selectivity for cancerous cells, these new compounds may provide increased DNA damage through the ferrocenium salts and antimetastatic qualities from the NAMI-A component of the compounds. By combining the therapeutic effects of these two complexes into one complex, cancer cells could be more selectively targeted and aptly combated with reduced side effects. Three complexes were synthesized, [Na][trans-$RuCl_4$(dmso)(pyrdyl-ferrocene)], [Na][trans-$RuCl_4$(dmso)(imidazolyl-ferrocene)], and [Na][trans-$RuCl_4$(dmso)(4 – ferrocenoyl-pyridine)] which will be referred to as RuL1, RuL2 and RuL3 respectively[35].

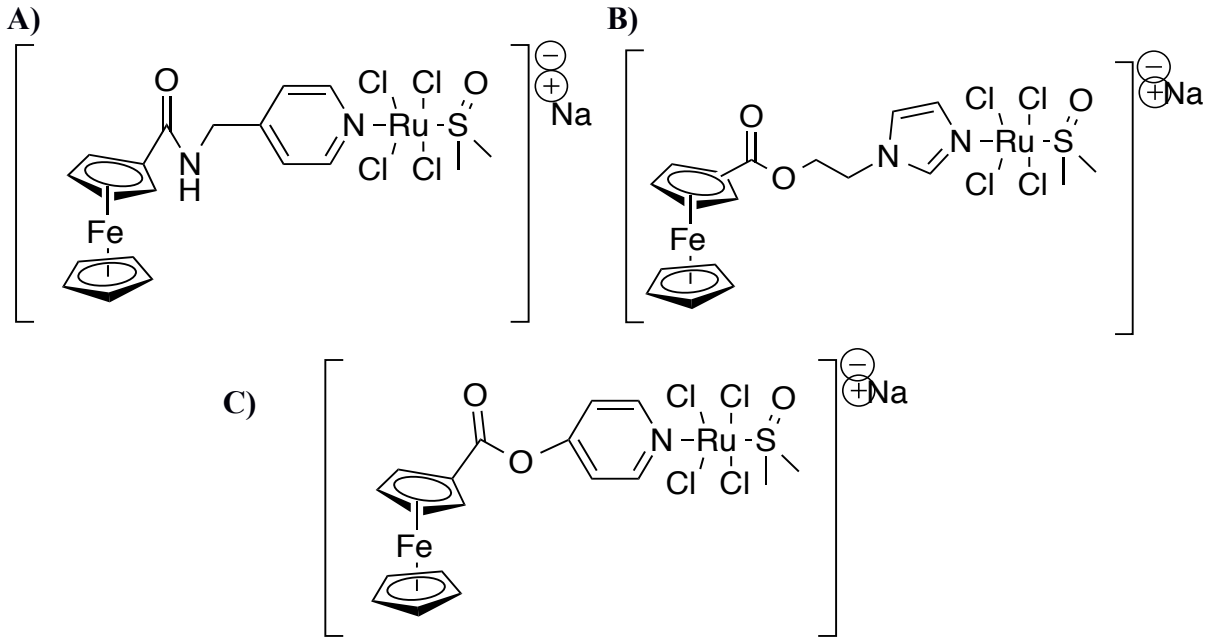

Figure 8: The chemical structures of the RuLX series of complexes. **A**) RuL1 **B**) RuL2 **C**) RuL3[27]

In electrophoretic mobility shift assays, all three compounds exhibited dose-dependent interactions with plasmid DNA comparable to cisplatin[35]. Moreover, when incubated with both human and bovine serum albumin proteins, all three complexes exhibited a dose-dependent affinity to the proteins visualized in native polyacrylamide gel electrophoresis (unpublished results). RuL3 in particular exhibited such a strong affinity that it appears to degrade the proteins after incubation at physiological temperatures[36]. Moreover, studies monitoring the obscuring of tryptophan's fluorescent signal due to RuLX interactions with BSA showed that all three complexes possess interactions with the BSA proteins[35].

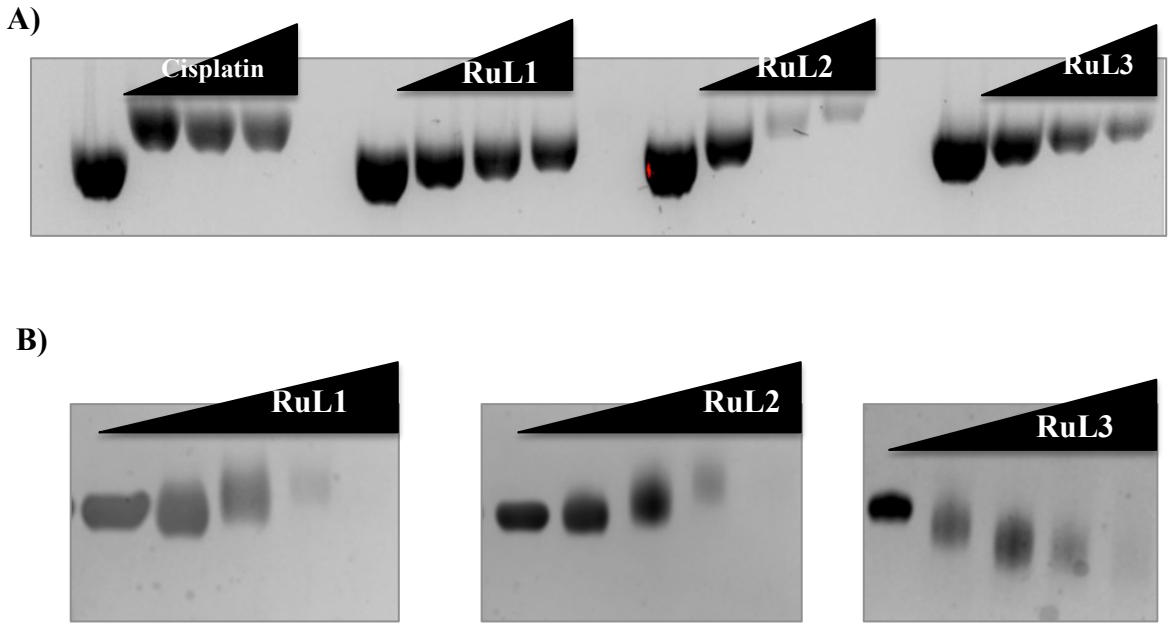

Figure 9: **A)** Agarose (1.5%) gel electrophoresis of cisplatin, RuL1, RuL2, & RuL3 treated DNA (1 μg) using various concentrations of each drug. The bands were visualized using ethidium bromide.[27] **B)** 8% Native-PAGE images where Bovine Serum Albumin incubated with RuL1, RuL2 and RuL3 in increasing concentrations[28].

Due to such evidence, the RuLX compounds are fitting candidates to investigate their binding potential to RNA, which is similar to DNA in chemical structure, and any potential downstream effects that may arise.

1.6. Translation inhibition as an anticancer target

Translation, the process in which cellular ribosomes build proteins using information garnered from messenger RNA, is an attractive target for cancer therapy due to its importance in the cell cycle. The fact that ribosomal subunits can self assemble *in vitro* from their constituent parts provided the ability to identify the roles of proteins and their processes during ribosome assembly and translation[37]. Protein synthesis takes place following assembly of both the 40*S* and 60*S* subunits onto the mRNA, and given the presence of charged tRNAs. The process of protein

synthesis goes as follows: Firstly, synthesis proceeds from the N-terminus to the C-terminus of the protein[37]. Secondly, the ribosomes read the mRNA in the 5' to 3' direction. Thirdly, active translation occurs on polyribosomes. This means that more than one ribosome can be bound to and translate a given mRNA at any one time[37]. Finally, chain elongation occurs by sequential addition of amino acids to the C-terminal end of the ribosome bound polypeptide. Translation proceeds in an ordered process[37]. First, accurate and efficient initiation must first occur, only then can chain elongation take place and finally, accurate and efficient termination is required to finish the job[37].

The initiation of translation occurs in four specific steps: first, ribosome must dissociate into its *40S* and *60S* subunits. Several initiation factors (e.g. eukaryotic translation initiation factor-1 [eIF-1] and eIF-3) are required to ensure that the 60*S* and 40*S* ribosomal subunits remain separated so that new rounds of translation can begin[37]. Then, the ternary complex−composed of GTP bound to the α-subunit of eIF2 and the initiator methionyl-tRNAmet, forms and engages the 40*S* subunit[37]. The eIF-4F complex−the mRNA activator for translation, which comprises the cap-binding factor, eIF-4E, the RNA helicase eIF-4A, and the scaffold subunit eIF-4G, captures mRNA and brings it to the 40*S* subunit and the ternary complex[37]. The mRNA then binds to the ternary complex and the *60S* subunit associates with the pre-initiation complex to form the *80S*, subunit thus completing of the process of translation initiation[37]. This key step in translation is an attractive anti-proliferative target as proteins synthesis cannot take place without it correct completion. Moreover, the plethora of proteins that are required to modulate this process provides ample targets for this task.

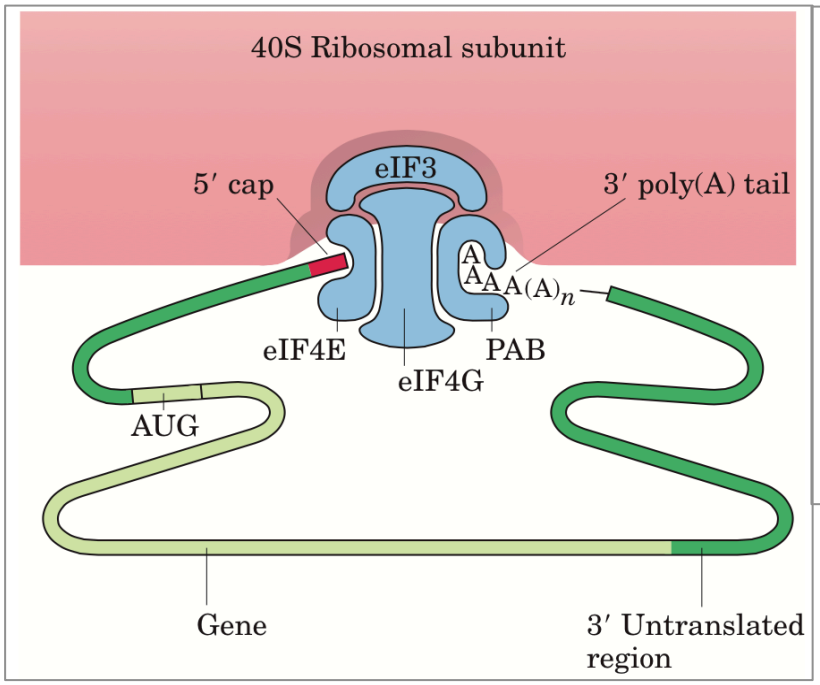

Figure 10: Protein complexes in the formation of a eukaryotic initiation complex. The 3'and 5' ends of eukaryotic mRNAs are linked by a complex of proteins that includes several initiation factors and the poly(A) binding protein (PAB). The factors eIF4E and eIF4G are part of a larger complex called eIF4F that binds to the 40S ribosomal subunit. [37]

One of the most recent targeted proteins for anti-proliferative properties is the eukaryotic translation initiation factor 4E (eIF4-E). EIF4-E is frequently overexpressed in human cancers when examined in relation to disease progression[38]. Its overexpression also drives cellular transformation, tumorigenesis, and metastatic progression in experimental models. Enhanced eIF4E function can be caused by eIF4E overexpression, and/or activation of the *ras* and phosphatidylinositol 3-kinase/AKT pathways[38]. This selectively increases the translation of key mRNAs involved in tumor growth, angiogenesis, and cell survival. Consequently, targeting eIF4E for inhibition may provide an attractive therapy for many different tumor types[38]. This is because reducing eIF4E expression simultaneously and selectively reduces the expression of other growth and survival factors critical for malignancy[38].

1.7. Silvestrol: a translation inhibiting anticancer compound

After it was found that the eukaryotic translation initiation factor 4E (*eIF4E)* is overexpressed in clinical cases of human cancers, as well as tumorigenesis, and metastatic progression in experimental models, considerable amount of research has been conducted targeting translation initiation inhibition as anti-cancer therapy. It was additionally found that eIF4E cooperates with c-Myc during lymphomagenesis to induce drug resistance, and is a genetic modifier of the rapamycin response[39]. The effect of dysregulation of the ribosome recruitment phase of translation initiation was also found to affect tumor progression and chemosensitivity[39]. A candidate drug, Silvestrol, a compound in a class of natural cyclopenta[*b*]benzofuran flavaglines was shown to enhance chemosensitivity in a mouse lymphoma model in which carcinogenesis is driven by phosphatase and tensin homolog (PTEN) inactivation or elevated eIF4E levels[39]. These results establish that targeting translation initiation could restore drug sensitivity *in vivo* and provide an approach to modulating chemosensitivity[39]. It was also shown that silvestrol is a potent anticancer compound *in vivo* as it inhibits the translation of malignancy-related mRNAs, affecting survival pathways and angiogenesis[40]. Silvestrol's mechanism of action is said to be that it promotes the dimerization of *eIF4A* with RNA, which disrupts efficient translation initiation[40]. This, in turn, inhibits protein synthesis and as a result, disrupts tumor survival pathways.

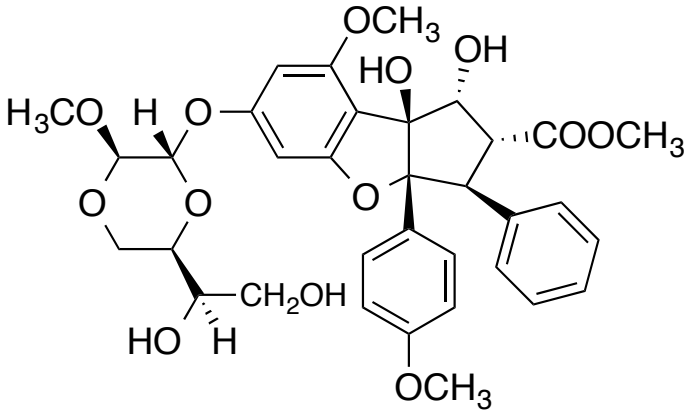

Figure 11: The chemical structure of Silvestrol

The potential of heteromultinuclear metal complexes to inhibit translation inhibition has seldom been discussed in recent research. The unselective nature of reactivity of metal

complexes with biomolecules makes metal complexes an attractive class of complexes to be studied for this purpose. Cisplatin has been implicated in *in vitro* translation inhibition by preventing the formation of the complete initiation complex and perhaps slowing down the process of chain elongation during translation[17]. The RuLX series of compounds have shown an affinity to bind both DNA and proteins, which begs the question: Do these complexes interact with RNA? If so, would this interaction interfere with the process of translation?

1.8. Experimental overview

To investigate the potential binding and inhibitory effects of the RuLX series of compounds, a model system using dihydrofolate reductase (DHFR) plasmid DNA was employed. DHFR plasmid was chosen not only due to its convenience−it is the control DNA provided by New England Bio labs Pure Express® *In Vitro* Protein Synthesis kit, but also due to that fact that it contained all the necessary information to be transcribed into RNA and translated into a detectable DHFR enzyme. Once acquired, the plasmid DNA will be amplified and digested in preparation for its transcription into RNA. Following transcription, the binding affinity of RuLX series of compounds to the resultant DHFR RNA will be investigated using an electrophoretic mobility shift (EMSA) assay. The EMSA assay is based on the observation that in agarose gel electrophoresis, heavier items migrate more slowly through the gel than lighter items. Thus, RNA successfully bound to any of the RuLX series of compounds will migrate more slowly than unbound RNA and difference in electrophoretic mobility would be evident. Moreover, this interaction should be evident in a dose-dependent manner as the greater the concentration of bound drug there is, the slower RNA migration.

Furthermore, downstream effects of RuLX-bound RNA will be investigated by comparing the translation efficiencies of DHFR RNA unexposed to the RuLX series of compounds versus the DHFR RNA that was exposed. Product presence will be detected using a DHFR assay that monitors the disappearance of NADPH, which has unique UV absorbance at 340 nm. DHFR catalyzes the reduction of 7,8-dihydrofolate to 5,6,7,8-tetrahydrofolate utilizing NADPH as a cofactor.

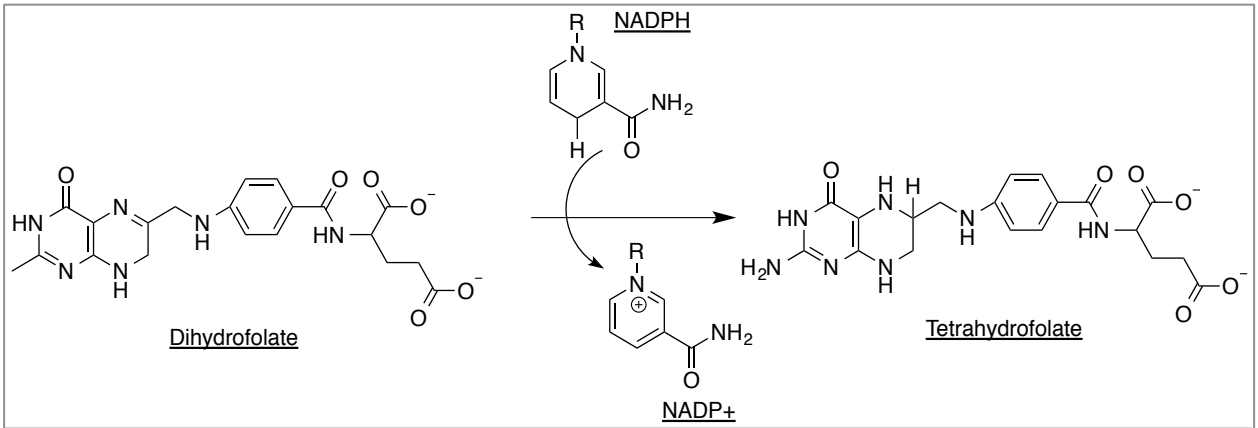

Figure 12: The reaction catalyzed by the enzyme dihydrofolate reductase using NADPH as its coenzyme.

Interestingly, within cells, this reaction is an essential step in the biosynthesis of nucleotide bases of DNA[41]. DHFR has also been considered as a target for anticancer drugs because its blockage in the cells causes apoptosis as a consequence of DNA synthesis inhibition[41-43]. Nevertheless, if exposure to the RuLX series of compounds prior to translation results in a reduction of DHFR activity, it is likely that the RuLX series of compounds can inhibit translation, at least *in vitro*. The RuLX series of complexes possess similar interactions with nucleic acids as ferrocenium salts and cisplatin. Hence, it is possible that they may also inhibit the *in vitro* translation of DHFR enzyme by binding to its mRNA.

2. Materials and Methods

2.1. Experimental roadmap

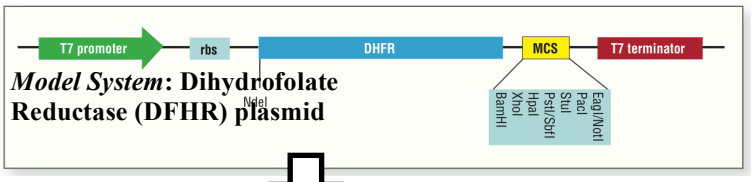

2.1-2.3 Plasmid amplification and extraction using *Escherichia Coli*

2.4 Restriction digestion of extracted DHFR plasmid with *StuI* and *BamH1* enzymes

2.5 *In vitro* transcription of DHFR linear DNA

2.6 Incubation of DHFR RNA with RuLX Complexes

2.7. Binding studies of RNA and RULX complexes via electrophoretic mobility shift assay

2.8. *In vitro* translation studies

2.9. Detection of translation product using a DHFR catalyzed reaction

2.10. Survey of translation inhibition using initial reaction rates to quantify DHFR produced using RuLX-incubated RNA

2.11. Important Controls I: Quantification of DHFR production using RuLX-incubated translation machinery

2.12. Important Controls II: Quantification of DHFR activity using RuLX incubated with pure DHFR enzyme

2.13 **Follow-up studies**: Inhibition of *in vitro* translation due to RuLX-RNA interactions

2.2. Transformation of Dihydrofolate Reductase (DHFR) plasmid into competent Escherichia Coli cells

Zymo® Mix & Go competent cells were thawed on ice and 2 µL of Dihydrofolate Reductase plasmid acquired from New England Bio labs Pure Express® *In Vitro* protein synthesis kit was added to the competent cells. After mixing gently for a few seconds 50 µL of the mixture was spread onto a pre-warmed (37°C) LB culture plate containing Ampicillin (100 µg/mL). The plate was incubated at 37°C overnight. A colony was harvested from the plate and grown, as a starter culture, on 5 mL of LB liquid media also containing Ampicillin (100 µg/mL) overnight to prepare for plasmid extraction. Starter culture was diluted 1/1000 into 200 mL of LB ampicillin (100µg/mL) containing liquid culture. The mixture was grown at 37°C for 16 hours shaking at 220 rpm.

2.3. Plasmid Extraction of DHFR plasmid using QIAGEN Plasmid Maxi Prep Kit[44]

Plasmid extraction was performed according to QIAGEN instructions with the following modifications[44]. The starter culture was shaken at 220 rpm instead of the recommended 300 rpm. The 7th Centrifugation step was conducted for 1 hour at 4 °C, instead of the suggested 30 minutes. The DNA was precipitated using ice-cold 100% ethanol instead of isopropanol and centrifuged as indicated by the QIAGEN maxi prep instructions.

2.4. Restriction Digestion (RD) of 10 µg of DHFR plasmid using the restriction enzymes

Table 1: Reaction Assembly of restriction digestion of 10 µg of DHFR plasmid

	Volume (µL)
DHFR plasmid (0.359 µg/µL)	28

10X NEB Buffer # 2	5
10 U *BamH1*or *StuI* enzyme (5 U/µL)	2
DEPC-treated H_2O	15
Total Reaction Volume	50

The above contents were thawed on ice, assembled in a fresh microcentrifuge tube, mixed thoroughly, and spun down to the bottom of the tube. After which, they were incubated at 37°C for 5 hours. The reaction products were purified using phenol chloroform extraction followed by ethanol precipitation.

Phenol: Chloroform Extraction was conducted as follows. One volume of Phenol: Chloroform: Isoamyl Alcohol (25:24:1) from Ambion was added to the restriction digestion product (50 µL). The mixture was vortexed for 30 seconds and then centrifuged for 2 minutes at 14000 rpm (top speed) 20° C. After, the upper, aqueous phase of the mixture was extracted and placed in a new microcentrifuge tube where one more volume of phenol: chloroform: isoamyl alcohol was added. It was vortexed for one minute and spun at top speed, 20°C for 2 minutes. Then, the upper, aqueous phase was, once again, transferred to a fresh tube. Any transferred chloroform was removed by centrifugation for 10 seconds at top speed followed by removal of the bottom phase with a micropipette. The resultant RNA solution was precipitated using ethanol precipitation.

Ethanol precipitation was conducted as follows. $1/10^{th}$ of reaction volume of 3 M sodium acetate (NaOAc) was added to the mixture (for a final concentration of 0.3M NaOAc) and mixed thoroughly. Then, three volumes of 100% ethanol was added to the resultant mixture and mixed thoroughly. The mixture was placed in -80°C freezer for 1 hour (to overnight) prior to centrifugation. The resultant microcentrifuge tube was centrifuged at 14000 rpm, 4°C for 1 hour and its supernatant was discarded and the pellet was washed with 70% ethanol. After the 70% ethanol was discarded the tube was air dried for 10-20 minutes and then re-suspended in 30µL

TE buffer. A 1:25 dilution was made in TE buffer for UV quantification of RD product and a diagnostic 1% agarose gel comparing circular DHFR DNA and linearized DHFR product was also prepared to ensure proper linearization.

2.5. *In Vitro* Transcription (TXN) of DHFR DNA

Table 2: Reaction assembly of a preparative scale *in vitro* transcription of DHFR DNA

	Amount (µL)
DEPC H_2O	10
10X Transcription Buffer (400 mM Tris-HCl, 60 mM $MgCl_2.6H_2O$, 100mM DTT)	10
10X (25 mM) Ribonucleotides	10
Linear DNA template (0. 976 µg/µL, 1.08 µM)	10
Inorganic Pyrophosphatase (0.1 U/µL)	5
T7 RNA Polymerase	25
TOTAL	100 µL

The above ingredients were thawed on ice and assembled, as written, at room temperature and in a new microcentrifuge tube; the mixture was then incubated at 37 °C for 3 hours.10U of TURBO DNase was then added to the mixture and incubated at 37°C for an additional 30 minutes. To stop the reaction, 5 µL of 500mM EDTA was added to the mixture

The mixture was then purified using phenol: cholorform: isoamyl alcohol and precipitated using ethanol as aforementioned in the previous section.

2.6. Preparative incubation of RNA with RuLX complexes

Table 3: Reaction assembly of preparative scale incubations of RuLX with RNA

	0 µM	**5 µM**	**50 µM**	**250 µM**	**500 µM**
RNA (µg/µL)	10 µL	10 µL	10 µL	10 µL	10 µL
RuLX	----	2 µL✪	2 µL⊙	1 µL○	2 µL○
TE Buffer	10 µL	8 µL	8 µL	9 µL	8 µL
TOTAL	20 µL	20 µL	20 µL	20 µL	20 µL

- From 5 mM Stock RuLX
- From 0.5 mM Stock RuLX
- From 0.05 mM Stock RuLX

The above materials were incubated at 37°C for 3 hours . After incubation, the mixtures were aliquoted (4 aliquots of 2 µL each, 2 aliquots of 6 µL) for future translation and stored in -80° C freezer.

2.7. Binding studies of RuLX complexes with DHFR RNA using an electrophoretic mobility shift assay

1-1.3% agarose gels were prepared where previously incubated samples (6 µL aliquots) were run using Bio-Rad's Sub-Cell® agarose gel electrophoresis systems at appropriate voltages.

2.8. *In Vitro* Translation (TSN) of DHFR plasmid

Table 4: Reaction assembly of a representative *in vitro* translation (TSN)

	Control DNA	**No Reaction**	**TSN**
Solution A	5 µL	5 µL	5 µL
Solution B	3.75 µL	3.75 µL	3.75 µL
Nuclease-free H_2O	2.75 µL	3.75 µL	2.75 µL
Template RNA	1 µL	0 µL	1 µL
TOTAL	12.5 µL	12.5 µL	12.5 µL

The mixture was assembled as written and incubated at 37°C for 3 hours. After incubation the mixture was stored in -21°C freezer until the DHFR activity assay was conducted

2.9. Detection of translation product: DHFR activity assay[45]

The assay was conducted following Sigma-Aldrich's DHFR assay kit using the following schemes and subsequent specifications:

Table 5: Reaction schemes followed when using the DHFR assay				
Reaction	**Assay Buffer 1x (µL)**	**Sample**	**NADPH (µL)**	**Dihydrofolic Acid (µL)**
Blank I	984	10 µL	6	------
Blank II	985	10 µL	-----	5
DHFR enzyme	979	10 µL (0.040 mg/mL) of DHFR enzyme	6	5
'No RXN'	981	6 µL of translation product without nucleic acid input	6	5
'Control DNA'	981	6 µL of translation product resulting from DHFR plasmid	6	5
'TSN3'	981	6 µL of translation product resulting from DHFR mRNA	6	5

The Cary UV spectrophotometer was set to collect a scan ranging from 290 nm to 410 nm, approximately every 25 seconds for five minutes. The reaction was set at 22°C using the block temperature control.

2.10. *Survey of translation inhibition*: RNA and RuLX Translation Inhibition Studies

Table 5: Reaction assembly of *in vitro* translations used in the survey of translation inhibition:					
	0 µM	**5 µM**	**50 µM**	**250 µM**	**500 µM**
Solution A	5 µL	5 µL	5 µL	5 µL	5 µL
Solution B	3.75 µL	3.75 µL	3.75 µL	3.75 µL	3.75 µL
Nuclease-free H_2O	1.75 µL	1.75 µL	1.75 µL	1.75 µL	1.75 µL
Template RNA-RuLX	2 µL	2 µL	2 µL	2 µL	2 µL
TOTAL	12.5 µL	12.5 µL	12.5 µL	12.5 µL	12.5 µL

The mixture was assembled as written above and incubated at 37°C for 3 hours. After incubation the mixture was stored in -21°C freezer until ready to use in DHFR assay. A DHFR assay of resultant translation products of RNA-RuLX complexes was conducted using Sigma-Aldrich Corp's[45] protocol using the following reaction schemes and subsequent changes:

Table 6: Reaction Schemes used in the survey of translation inhibition

Reaction	Assay Buffer 1x (µL)	Translation Product (µL)	NADPH (µL)	Dihydrofolic Acid (µL)
0 µM	981	6	6	5
5 µM	981	6	6	5
50 µM	981	6	6	5
250 µM	981	6	6	5
500 µM	981	6	6	5

Initial studies were conducted where the Cary UV spectrophotometer was set to collect a scan ranging from 290 nm to 410 nm, approximately every 25 seconds for five minutes. The reaction was set at 22°C using the block temperature control. Subsequent studies were conducted where Cary UV spectrophotometer was set to collect the absorbance at 340 nm approximately every 12 seconds for five minutes. The reaction was set at 22°C using the block temperature control.

2.11. *Important Controls I*: Quantification of DHFR production using RuLX-incubated translation machinery

Table 7: Reaction assembly for incubation of RuLX complexes with ribosomal proteins

	Control (0 µM RuLX)	80 µM RuLX
Solution A	5 µL	5 µL
Solution B	3.75 µL	3.75 µL
Nuclease-free H_2O	3.75 µL	0.75 µL
Template RNA	1 µL	1 µL
RuLX	---	2 µL
TOTAL	13.5 µL	12.5 µL

The mixture, without RNA, was assembled as written and incubated at 37°C for 3 hours. After incubation RNA was added to the appropriate samples and set, once more at 37°C for 3 hours. Thereafter, the mixture was stored in -21°C freezer until ready to conduct the DHFR activity assay. DHFR assay of resultant translation products of RuLX-incubated translation machinery was conducted using Sigma-Aldrich Corp's[45] protocol using the following reaction

schemes and subsequent changes:

Table 8: Reaction schemes for DHFR assay of RuLX-treated ribosomal proteins

Reaction (rxn)	Assay Buffer 1x (µL)	Translation product (µL)	NADPH (µL)	Dihydrofolic Acid (µL)
Control (0 µM RuLX)	981	6	6	5
80 µM RuL1	981	6	6	5
80 µM RuL2	981	6	6	5
80 µM RuL3	981	6	6	5

Initial studies were conducted where the Cary UV spectrophotometer was set to collect a scan ranging from 290 nm to 410 nm, approximately every 25 seconds for five minutes. The reaction was set at 22°C using the block temperature control. Subsequent studies were conducted where the Cary UV spectrophotometer was set to collect the absorbance at 340 nm, approximately every 12 seconds for five minutes. The reaction was set at 22°C using the block temperature control.

2.12. *Important Controls II:* Quantification of DHFR production using RuLX incubated with pure DHFR enzyme

Table 9: Incubation mixture assembly of RuLX complexes and DHFR enzyme

	Control (0 µM RuLX)	80 µM RuLX
Pure DHFR (0.40mg/mL)	6 µL	6 µL
0.5 mM RuLX solution	---	2.4 µL
DEPC H_2O	9 µL	6.6 µL
TOTAL	15 µL	15 µL

The above mixture was incubated at 37°C for 3 hours. It was then stored in -20°C freezer overnight until ready for DHFR activity assay. DHFR assay of resultant translation products of RNA-RuLX complexes was conducted using Sigma-Aldrich Corp's[45] protocol using the following reaction schemes and subsequent changes.

Table 10: DHFR reaction scheme for RuLX-treated enzyme

Reaction (rxn)	Assay Buffer 1x (µL)	DHFR (µL)	NADPH (µL)	Dihydrofolic Acid (µL)
Control (0 µM RuLX)	974	15	6	5
80 µM RuL1	974	15	6	5
80 µM RuL2	974	15	6	5
80 µM RuL3	974	15	6	5

Initial studies were where the Cary UV spectrophotometer was set to collect a scan ranging from 290 nm to 410 nm, approximately every 25 seconds for five minutes. The reaction was set at 22°C using the block temperature control. Subsequent studies were conducted where the Cary UV spectrophotometer was set to collect the absorbance at 340 nm, approximately every 12 seconds for five minutes. The reaction was set at 22°C using the block temperature control.

2.13. *Follow-up Studies*: Inhibition of *in vitro* translation due to RuLX-RNA interactions

Follow-up studies were conducted using RuL2-incubated RNA in 0, 5, 50 and 250 µM concentrations of the drug. Triplet translations were assembled of each concentration according to aforementioned specifications (see Materials and Methods 2.110.). DHFR activity was monitored in likewise fashion. Moreover, a control measuring the effect of RuL2 incubation on pure DHFR enzyme was also set up in triplicate (see Materials and Methods 2.12.). DHFR activity was also measured for this set of experiments.

3. RESULTS

Successful amplification of plasmid DFHR DNA, digestion of said DNA and its *in vitro* transcription established the chosen model system as a successful system to investigate translation inhibition. Evidence suggests that RuL2 and RuL3 have a stronger binding affinity to RNA than RuL1. Furthermore, all three complexes exhibited a dose-dependent reduction of DHFR activity. Follow-up studies, with RuL2 specifically, suggest that its inhibition may be due to binding to RNA, binding to the translation machinery or binding to translation product, the DHFR enzyme itself. Explorative controls show that RuL2 does not significantly inhibit pure enzyme activity or ribosomal protein activity. Thus, it is likely that RuL2 interacts with the mRNA is such a way that it inhibits translation of a full-length, active DHFR enzyme.

3.1. Amplification, digestion and *in vitro* transcription of DHFR DNA

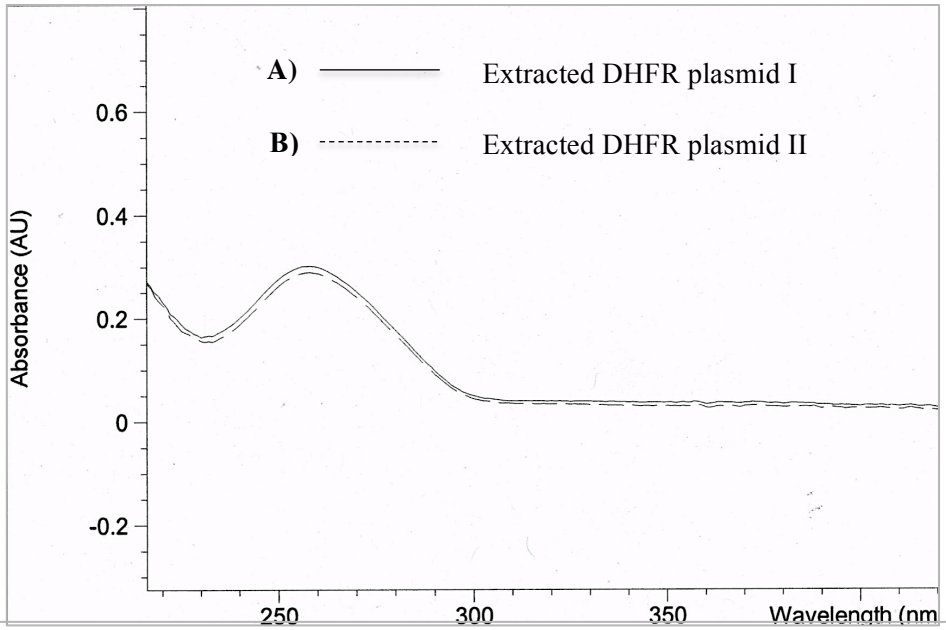

Figure 13: Representative graph of UV quantification of dilute (1:25) DHFR plasmid from *E. coli* to give the concentrations **A)** 0.375 µg/µL and **B)** 0.359 µg/µL. The fractions gave A260/A280 ratio of **A)** 1.70 and **B)** 1.72 respectively.

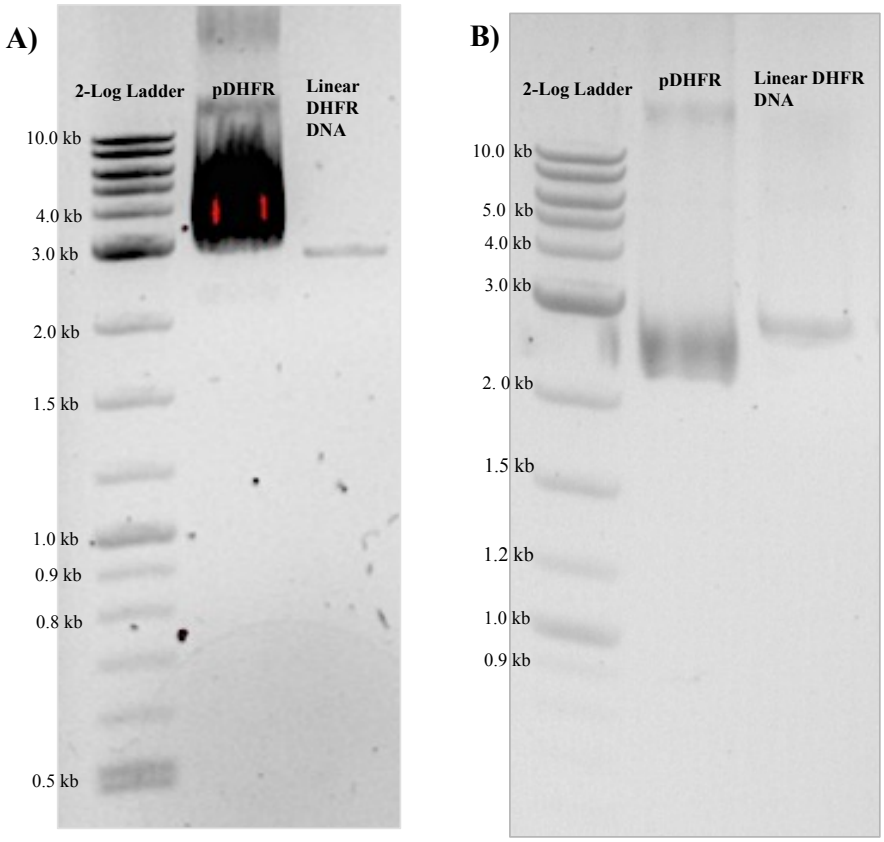

Figure 14: Representative agarose gels (1.0%) comparing plasmid DHFR DNA and linearized DHFR DNA were visualized using ethidium bromide. Both gels were run at 100V for 1 hr. **A)** Restriction digestion of 4 µg of plasmid DHFR using BamH1 enzyme. **B)** Restriction digestion of 1 µg of plasmid DHFR using *StuI* enzyme

To determine whether amplification of DHFR plasmid was successful, plasmid was extracted from transformed *E. coli* cells and quantified by measuring the solution's UV absorbance. It yielded two aliquots of plasmid DNA that are 0.375 µg/ µL and 0.359 µg/µL; the DNA was relatively pure as both aliquots had A_{260}/A_{280} ratios of 1.70 and 1.72 respectively – a small deviation from the ideal A_{260}/A_{280} of 2 (Figure. 13).

To check the extracted plasmid's length and to determine success of restriction digestion, agarose gel electrophoresis of both circular DHFR DNA and the restriction digested DNA was

conducted. Gel analysis also showed appropriate bands for plasmid DHFR DNA; the band was near ~3000 base pairs which was congruent with the length of the DHFR plasmid which is 2879 base pairs (Figure. 14). Dense bands evident in the plasmid DNA lane are most likely due to overloading of the well with DNA and perhaps some of its smearing can be attributed to the degradation of some of the DNA (Figure. 14A). However, once digested with *StuI* and purified, degraded DNA was discarded and the resultant linear DNA showed greater band quality when run on an agarose gel (Figure. 14). Furthermore, the linearized DNA migrated slightly slower than the plasmid DNA indicating that it is, in fact, linear (Figure 14B). Plasmid DNA migrates slower than linear DNA due to the superhelical tension of its confirmation.

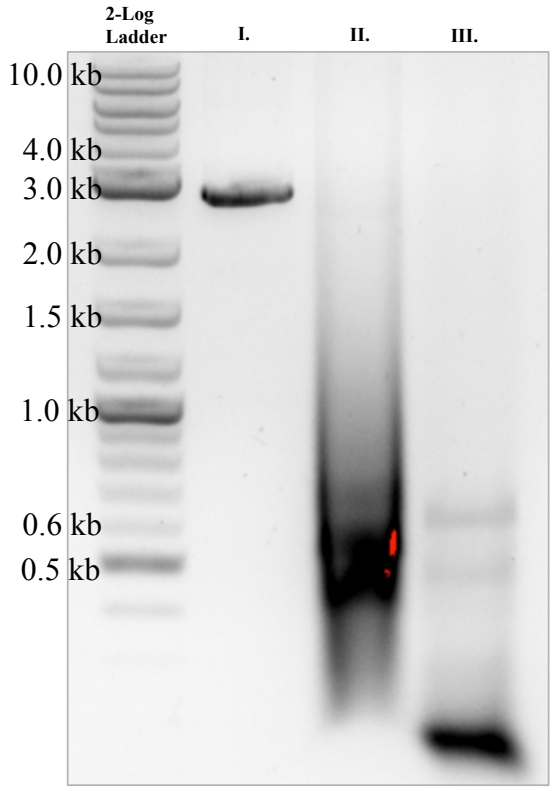

Figure 15: Diagnostic agarose gel (1.0%) visualized using ethidium bromide. Both gels were run at 100V for 1 hour **I.** Linear DHFR DNA, **II.** Product of *In Vitro* Transcription, and **III.** RNAse A-digested *In Vitro* Transcription Product.

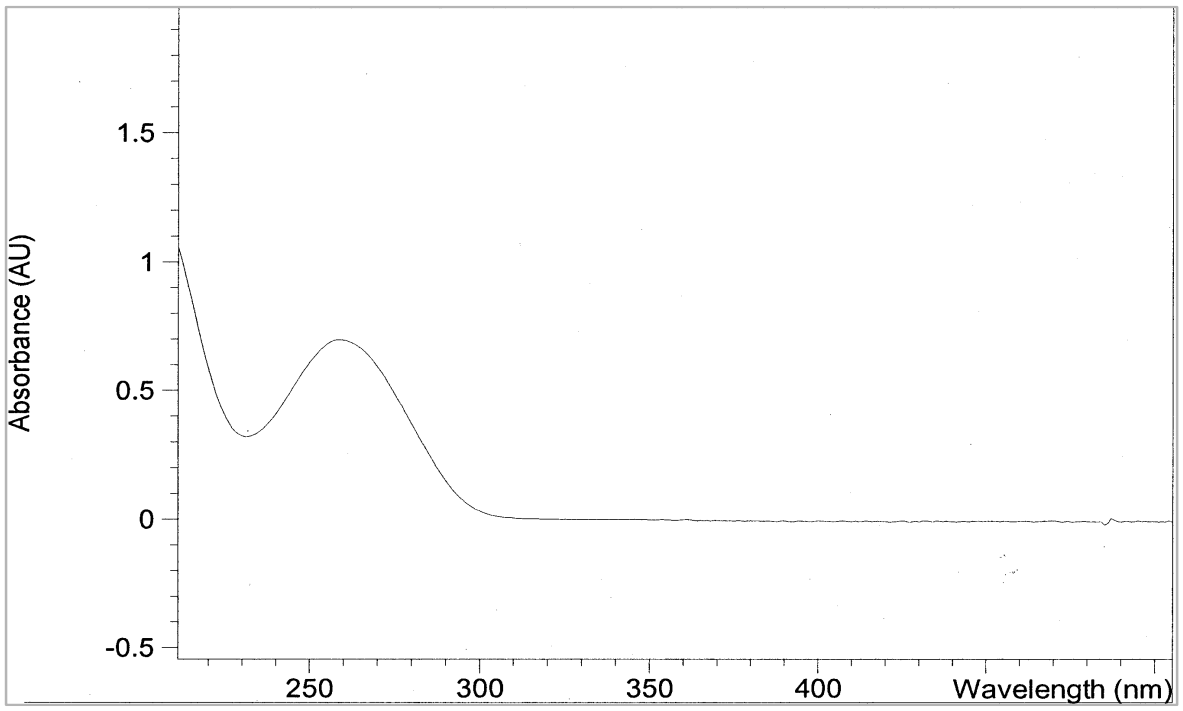

Figure 16: Representative graph of UV detection of 0.667 μg/μL RNA at 260 nm. Its A260/A280 ratio was 1.89. Samples were diluted 1:25 in DEPC-treated H_2O

To determine the success of *in vitro* transcription, agarose (1%) gel electrophoresis comparing the linear DHFR DNA to the transcription product and to the transcription product digested with RNase A was performed. The success of the *in vitro* transcription was ascertained due to the fact that the transcription product showed no presence of the DHFR DNA (~3000 base pairs) when analyzed by agarose gel electrophoresis (Figure 15I, 15II). The presence of a strong band at ~500 base pairs, congruent with the length of the DHFR mRNA which is 504 bases in length showed successful transcription of the DHFR mRNA (Figure 15II). Moreover, the transcription product is successfully digested by RNase A as evidenced by the disappearance of the band at ~500 base pairs and the presence of digested RNA in lengths shorter than 500 base pairs (Figure 15III). The mRNA product was detectable by UV and considerably pure with a A_{260}/A_{280} ratio of 1.89 (Figure 16).

3.2. *In Vitro* Translation and detection of DHFR activity

A)

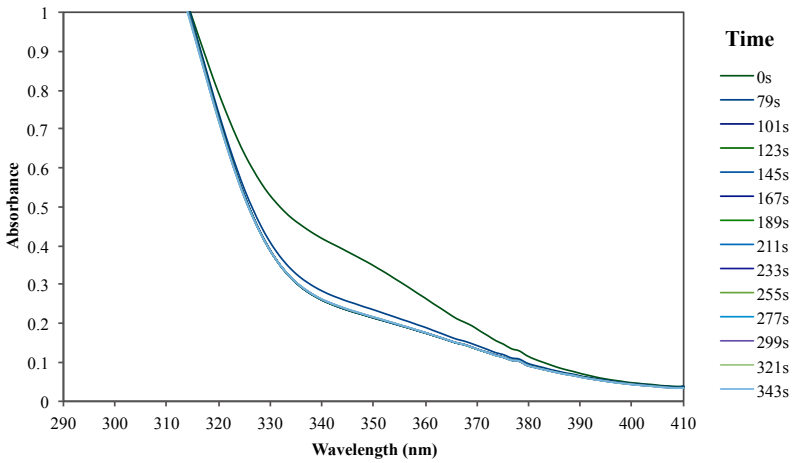

B)

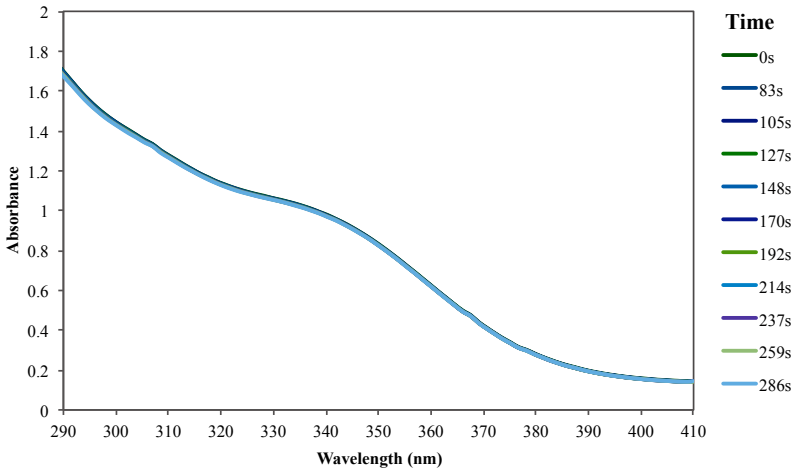

C)

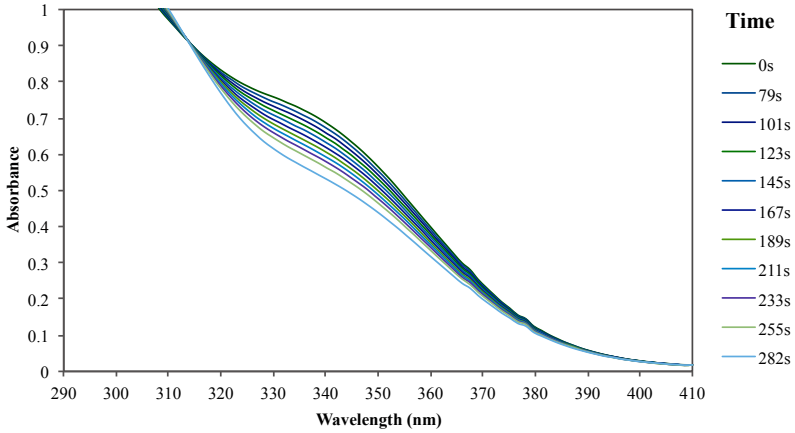

Figure 17: The depletion NADPH monitored by observing decay of 340 nm peak. **A)** Activity of translation product resultant from control DHFR DNA **B)** Activity of translation product without input of nucleic acid **C)** Activity of translation product resultant from DHFR mRNA obtained from *in vitro* transcription.

To determine whether successful translation of DHFR mRNA into an active, full-length DHFR enzyme occurred, three translation reactions were assembled. Each reaction contained either plasmid DFHR DNA obtained from the Pure Express® translation kit, 504-base DHFR mRNA obtained from in-house transcription, or no nucleic acid input. DHFR enzyme production was measured by monitoring the depletion of NADPH using its distinct absorbance at 340 nm. The rate of NADPH depletion is used as a quantifying reporter of the presence of full-length, active DHFR enzyme produced from *in vitro* translation. The faster the NADPH is consumed in the assay, the more DHFR enzyme is present in the translation product. A clear reduction in absorbance at 340 nm is evident from the resultant data (Figure 17). It is important to note that because proteins absorb at 280 nm, there is an obscuring of the signal at 340 nm by the intense protein absorbance resulting from not only the DHFR enzyme translated, but also from the ribosomal proteins responsible for the translation itself. However, the isosbestic points at ~314 nm and ~400 nm describe a two-state process and thus an adequate measure of NADPH disappearance.

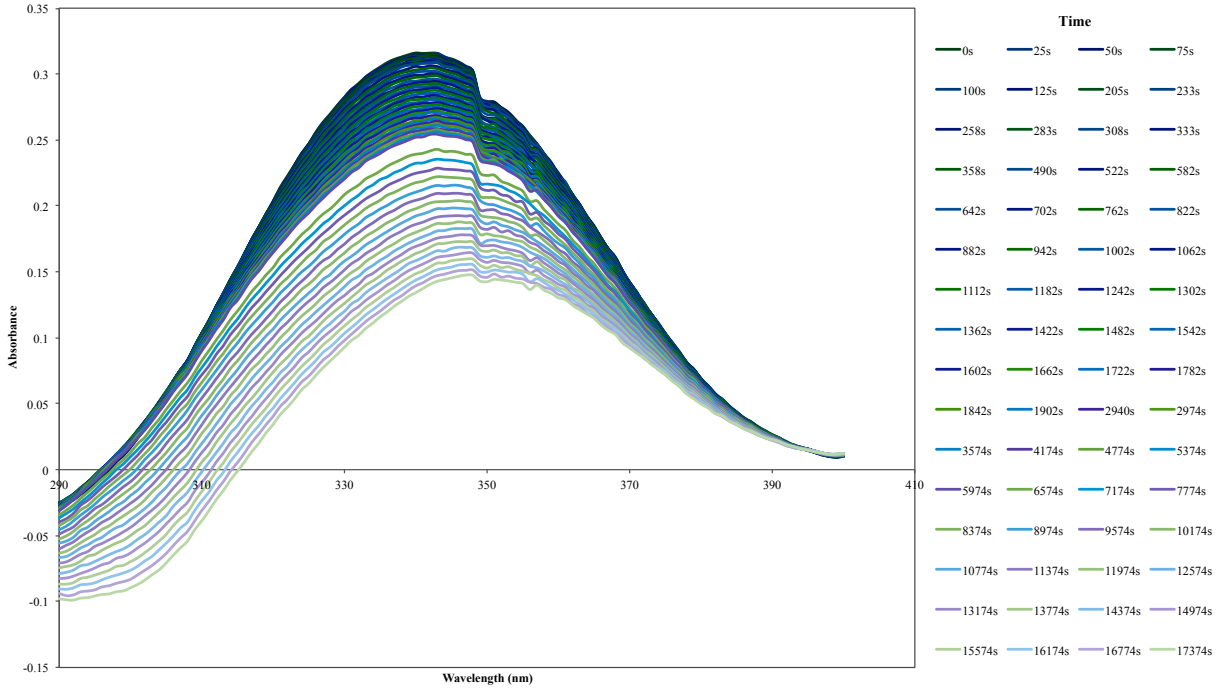

Figure 18: Baseline corrected UV spectral analysis monitoring the depletion of NADPH using 0.0040 mg/mL DHFR over 3 hours. Baseline reading was obtained from the UV analysis of all DHFR assay ingredients with the exception of NADPH (*See Blank II of Materials and Methods section 2.9).*

Nevertheless, a possible way to combat this obscuring of signal is to record a baseline correction reading using all the assay components except NADPH. A small sample of DHFR enzyme when measured using the aforementioned baseline correction, showed a considerable reduction in obscuring (Figure 18). Unfortunately, this baseline correction proved difficult to reproduce during subsequent trials, and thus was abandoned. However, because our analysis requires only the respective initial reaction rates to report the amount of DHFR produced, observing the depletion in the peak at 340 nm, regardless of obscuring, is still acceptable.

The DHFR mRNA appears to produce less enzyme compared to the DHFR plasmid DNA provided by the *In Vitro* Translation Pure Express ® Kit. This is evident in the significant

decrease in absorbance for the enzyme activity yielded by translating the DNA; it fell from 0.416 to 0.260 absorbance units in 79 seconds. The enzyme activity yielded by translating DHFR mRNA (obtained via in-house *in vitro* transcription) fell from 0.684 to 0.671 in the same amount of time (Figure 17A, Figure 17C). This suggests that there is larger quantity of DHFR enzyme produced by the translation reaction using DNA provided by the kit. Since the kit can translate full-length proteins given either DNA or RNA as input, it possesses the ability to conduct both transcription and translation. It is likely that these processes are coupled[48]. This produces a greater quantity of enzyme when DNA is used[48]. Nonetheless, successful translation of the DHFR mRNA into the active enzyme indicates that the DHFR assay is still a successful model system to investigate the process of translation and its inhibition.

Measuring the inability to produce full-length product, using DHFR mRNA as our input, can be used as a reporting system for investigating translation inhibition. Furthermore, the Pure Express ® *in vitro* translation system is an appropriate model system to investigate translation inhibition due to the fact that none of the ribosomal proteins that compose the translation machinery consume NADPH when tested in the DHFR assay. This was ascertained by the lack of change when the ribosomal proteins lacking in nucleic acid input were investigated using the DHFR assay (Figure 17B). All in all, the DHFR enzyme activity can be used as a reporter of the amount of DHFR produced by the translation system because not only does Pure Express ® *in vitro* translation kit produces active DHFR detectable by a DHFR assay, but also its components do not consume NADPH.

3.3. Binding studies using electrophoretic mobility shift assay

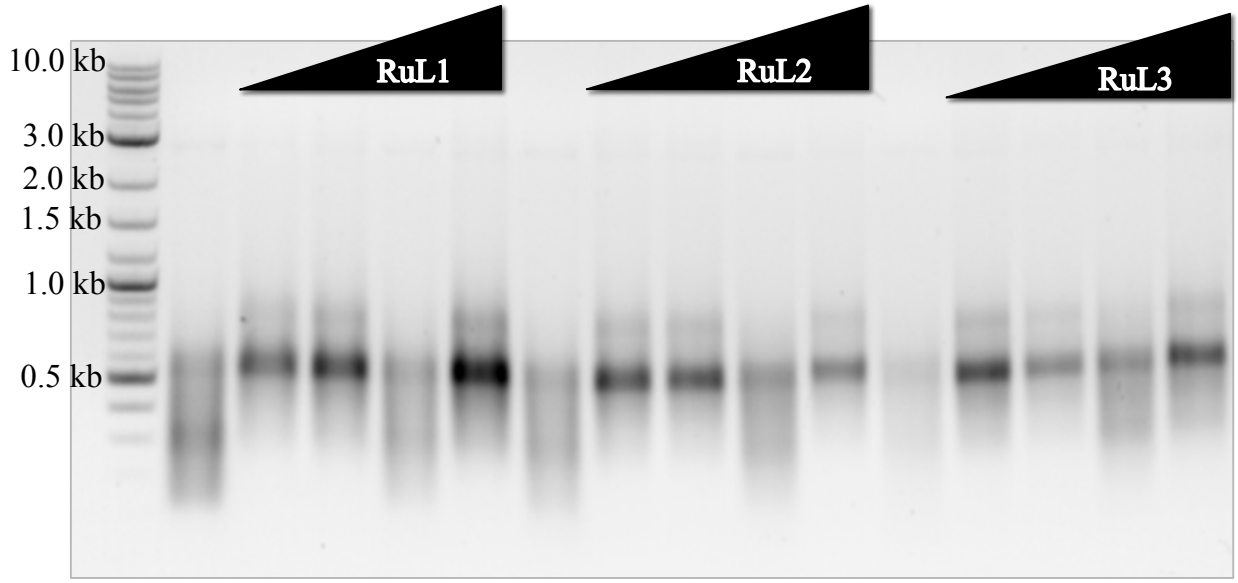

Figure 19: Agarose (1.0%) gel electrophoresis of RuL1, RuL2, & RuL3 treated RNA (3 μg) with increasing concentrations of each drug: 5, 50, 250, 500 μM. RNA was incubated with RuLX complexes for 3 hours. Gel was run at 100V for 1 hour.

To determine whether the RuLX complexes exhibit chemical interactions with RNA, DHFR mRNA obtained from *in vitro* transcription was incubated with various concentrations of the RuLX complexes. An electrophoretic mobility shift assay was used to visualize the chemical interactions resultant from the incubations. Our results suggest that RuL1 has the least interaction with RNA; RuL2 appears to have a more pronounced interaction, while RuL3 shows the most robust interaction with RNA. RuL2 and Rul3 incubated RNA showed a dose-dependent slowing in migration due to RNA-RuLX interactions (Figure 21).

In the first gel image, the difference in migration appears to be minute and the RNA bands migrated in smear patterns and with varying band density, both of which could be indicative of RNA degradation (Figure 19).

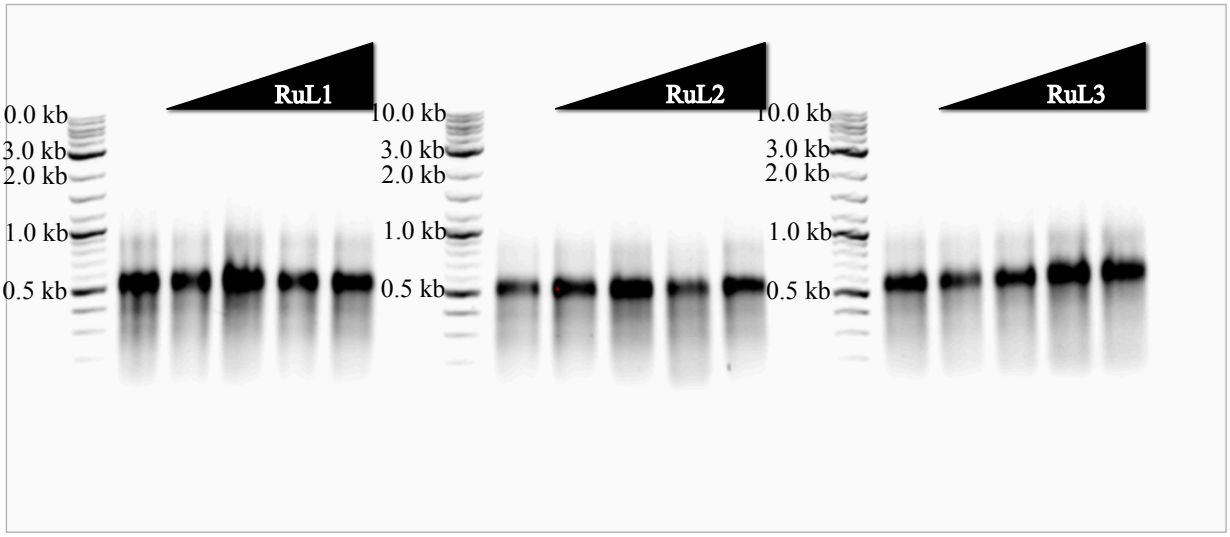

Figure 20: Agarose (1.0%) gel electrophoresis of RuL1, RuL2, & RuL3 treated, newly transcribed RNA (3 μg) using increasing concentrations of each drug: 5, 50, 250, 500 μM. RNA was incubated with RuLX complexes for 1.5 hours. Gel was run at 100V for 1 hour.

For the next set of experiments, a new transcription of RNA was carried out and incubated with the RuLX complexes for half the duration (1.5 hours) in hopes of alleviating degradation effects. The incubation mixture was run on an agarose gel at the same voltage and time as the previous experiments (Figure 20). These results show that while the RNA bands ran with constant density, the smearing persisted. This smearing is likely an artifact of the phenol-chloroform purification process where some of the RNA may have underwent phenol contamination and as a result, degraded (Figure. 20). Nonetheless, the migratory pattern persisted where RuL2 and RuL3 show the most promising interactions with RNA (Figure 20). Moreover, for better resolution, the experiment was repeated using higher percentage agarose (1.3%) and using the revised RNA and RuLX complex incubation time of 1.5 hours. The gel was also run for a longer time (4.5 hours) and at a lower voltage to ensure that heat generated from the electrophoresis apparatus did not impair any RuLX-RNA interactions (Figure 21). The resultant gel showed a step-wise slowing in migration from 50-200 μM concentrations of RuL2 and RuL3.

RuL1 did not show a slowing in migration of RNA even at this higher resolution (Figure 21). From the evidence garnered, it is likely that RuL2 and RuL3 are the only complexes possessing strong enough chemical interactions with RNA to survive agarose electrophoresis. It is possible that RuL2 and RuL3 form covalent adducts with the mRNA; however mass spectrometry studies are needed to confirm this hypothesis.

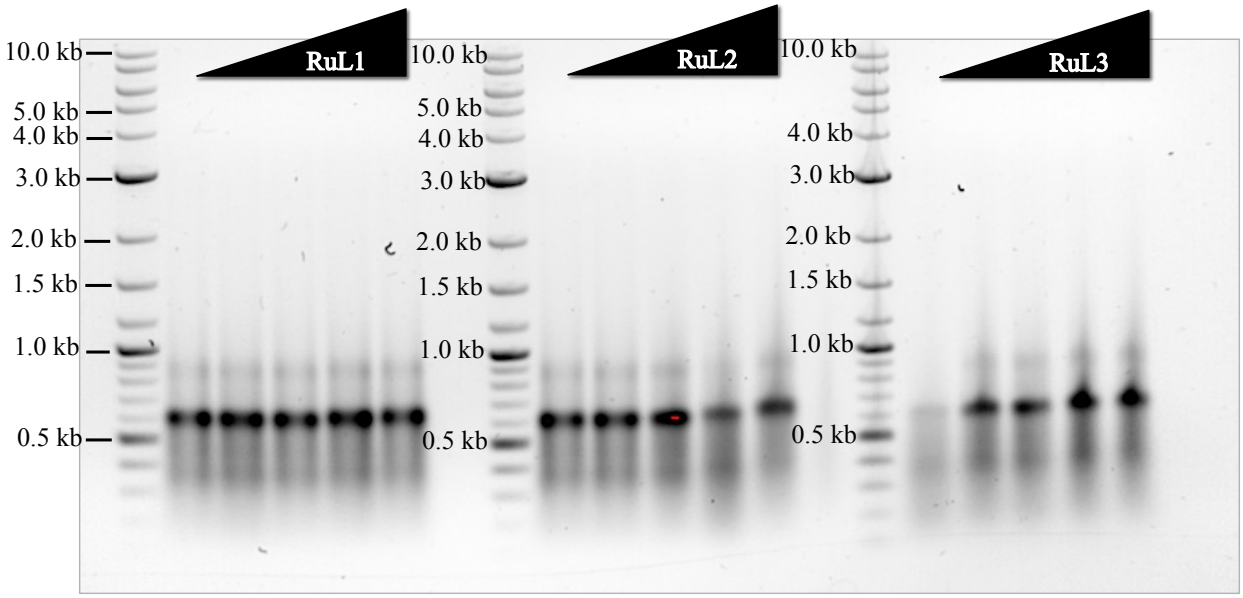

Figure 21: Agarose (1.3%) gel electrophoresis of RuL1, RuL2, & RuL3 treated RNA (2 µg) using increasing concentrations of each drug: 5, 50, 250, 500 µM. RNA was incubated with RuLX complexes for 1.5 hours. Gel was run at 50V for 4.5 hours.

RuL2- and RuL3-dependent slowing of RNA migration in agarose gel electrophoresis may be due to their distinct chemical structure as compared to RuL1. RuL2 and RuL3 both contain an ether moiety that bridges the NAMI-A-like and the ferrocene-like elements of their structures, while RuL1 possesses an amine group in that location (Figure 8). This could yield unique possibilities of reactivity for the RuL2 and RuL3 complexes that may not be available for the RuL1 complex. Anti-cancer compounds like Bisulfan are DNA alkylators containing the ether moieties that cause intrastrand cross-links between guanine bases in DNA double-helix

strands, directly attacking DNA[46]. RuL2 and RuL3's superior interaction with RNA compared to RuL1 could be due to similar alkylating mechanisms with RNA.

Furthermore, RuL2 contains an imidazole moiety that has been shown to favor reactivity with nucleic acids. The imidazole ring has been shown to be extremely reactive with biological molecules, in the reactivity it possesses especially as an integral component of the amino acid histidine, and its biological reactions. Moreover, imidazole's antiproliferative and antimetastatic contributions are evident in the success of NAMI-A as a candidate drug.

However, the nature of the RNA-RuLX interactions remains unclear. It is possible that the interactions are covalent due to the stability of RuLX-RNA interactions under the pressure of agarose gel electrophoresis. However more rigorous methods of study are needed to provide evidence for this. Particularly, inductively coupled plasma mass spectrometry and matrix-assisted laser desorption/ionization time-of-flight (MALDI-TOF) mass spectrometry experiments can shed great insight into these interactions. Using the aforementioned studies, NAMI-A was found to form adducts with RNA at comparable frequencies to which it forms adducts with DNA[47]. Moreover, MALDI-TOF studies also showed that when interacting with nucleic acids, NAMI-A bound to oligonucleotides with strong coordination with either a single ruthenium atom or a ruthenium atom linked to an imidazole ring[47]. It could be possible that the NAMI-A-like portion of the RuLX complex coordinates with RNA using similar mechanisms. Mass spectrometry studies can reveal more about the nature of these interactions than gel electrophoresis.

3.4. Survey of RuLX inhibition of RNA directed *in vitro* translation

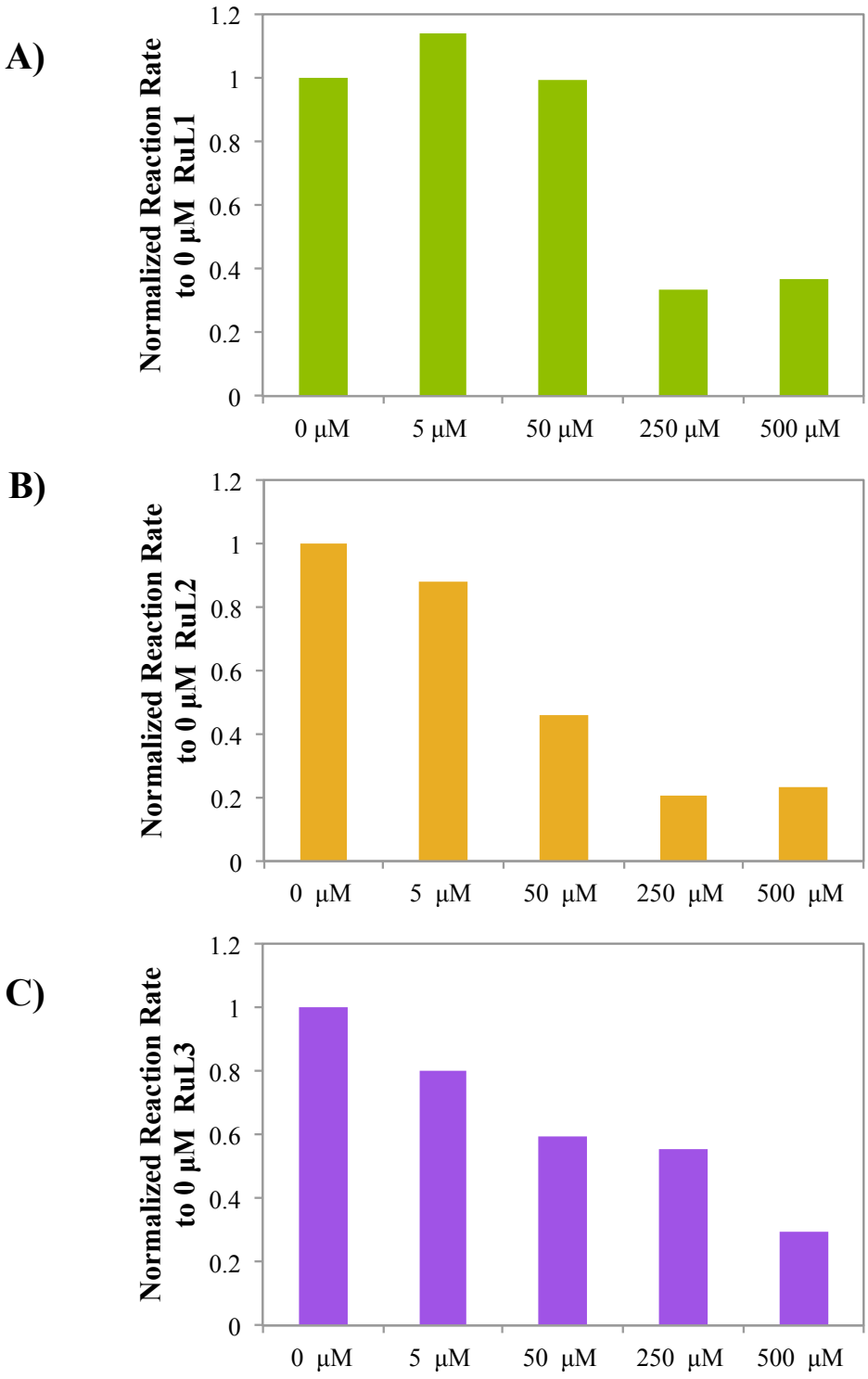

Figure 22: A survey of RuLX translation inhibition. Normalized rate of reaction of *in vitro* translation product using **A)** RuL1-treated RNA **B)** RuL2-treated RNA **C)** RuL3-treated RNA

To explore the inhibitory effects of the RuLX compounds during *in vitro* translation, a series of translation reactions were prepared using DFHR mRNA incubated with varying concentrations of RuLX complexes. Thereafter, their translation products were examined using a DHFR activity assay. The results of these studies suggest that there is a dose-dependent inhibition of translation for all three complexes (Figure 22).

RuL1-treated RNA shows a significant reduction in DHFR activity at a concentration of 250 μM and onwards, with a reduction of over half the activity when compared to translation using untreated RNA (Figure. 22). It also shows a counter-intuitive spike at concentrations of 5 μM and 500 μM RuL1 (Figure 22A). It seems as though there is more activity from DHFR resultant from RNA treated with 5 μM RuL1 than untreated RNA (Figure. 22A). This is likely a result of an experimental error; the experiment should be repeated multiple times to remedy this. Similarly, it seems as though there is slightly more enzyme activity of DHFR translated from RNA treated with 500 μM RuL2 than with RNA treated with 250 μM RuL2 (Figure 22B). This is likely an artifact to the natural variability of the translation machinery. Although incubated with the same components, in each new translation event, the translation machinery produces varying amounts of DHFR RNA. This was demonstrated in that different translation events with untreated RNA set up on the same day resulted in varied enzyme activity profiles. Moreover, it could be that at 250 μM, all the possible sites of interaction on the DHFR mRNA are occupied; this could be the concentration at which the DHFR mRNA is saturated with RuLX complexes. Nevertheless, a more statistically robust exploration of the enzyme activity yielded from the translation of RuL2-treated RNA is needed to account for variability of the translation output and assign statistical significance to the trend.

RuL2-treated RNA shows a plunge in DHFR activity at concentrations as low as 50 µM, where there is less than half of the activity compared to untreated RNA (Figure 22B). The reduction in activity appears to be dose-dependent, with the 250 µM having only a 1/5th of the activity that DHFR produced from untreated RNA has (Figure 22B). Likewise, RuL3 shows a significant reduction in DHFR activity by 50 µM, where there is a 40% reduction in DHFR activity (Figure 22C). Dose-dependency is evident because enzyme activity decreases as the concentration of RuLX complexes increases (Figure 22C). However, more statistically robust explorations of these interactions are needed to assign statistical significance to the inhibition and to establish the concentration at which there is a significant reduction in activity for each complex. This would provide insight as to which complex is more effective at inhibiting RNA driven *in vitro* translation.

3.5. Important controls to investigate nature of the translation inhibition

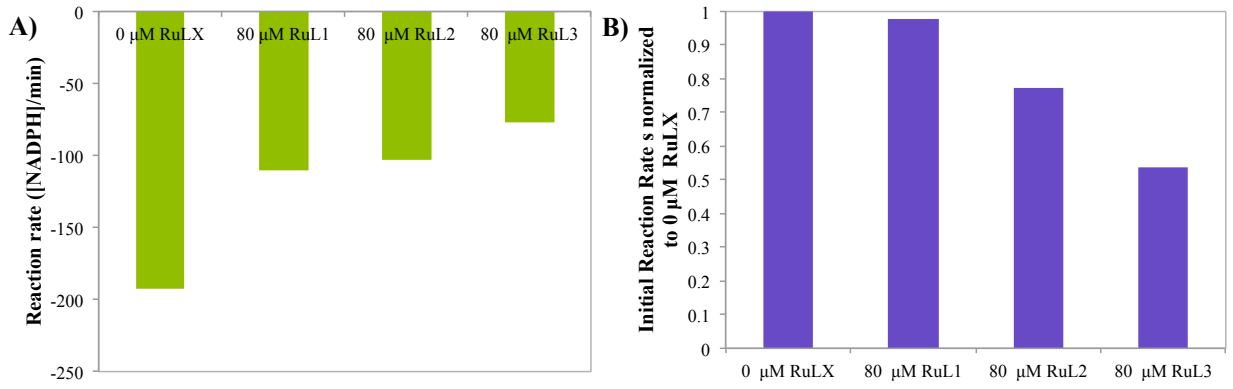

Figure 23: Important controls to investigate the nature of inhibition **A)** Enzyme activity of ribosomal proteins with 80 µM of RuLX complexes and supplied with DHFR mRNA for translation **B) Activity of** DHFR enzyme incubated with 80 µM of RuLX complexes.

To ensure that the inhibition measured by the depletion of NADPH is due to the impairment of translation by RNA-RuLX interactions, two controls were designed to tackle

potentially confounding interactions between the RuLX complexes and proteins. Due to the fact that previous work has shown that the RuLX complexes can chemically interact with both DNA and proteins, it is important to establish a control to ensure that the reduction of enzyme activity is not due to RuLX interactions with the ribosomal proteins or RuLX-induced impairment of successfully translated, active, full-length DHFR.

To investigate whether the RuLX complexes inhibit efficient translation by impairing the ribosomal proteins, ribosomal proteins were incubated with the highest exposure of RuLX complexes for 3 hours and used in translation reactions that utilized clean DHFR mRNA as their input. The highest exposure of RuLX to the ribosomal proteins was calculated to be 80 μM, which corresponds to 500 μM RuLX-treated RNA. This is because when the RuLX-treated RNA is entered into the translation reaction assembly, the overall concentration of RuLX complexes exposed to the ribosomal proteins is diluted. The results of this survey suggest that the complexes do interact with the translation machinery inhibiting efficient translation in an unidentified fashion (Figure 23A). After incubation with all three complexes, RuL1 and RuL2 exhibit half the rate of NADPH consumption of the DHFR obtained un-incubated translational machinery. RuL3 shows the most significant reduction of DHFR activity and thus, it is likely that it is the mechanism that contributes the bulk of the inhibitory effects of the complex (Figure 23A). However, due to minimal materials and lack of time only an exploratory investigation of these effects was conducted; a more robust investigation of the complexes is needed to delineate not only whether the contribution of RuLX interactions with the ribosomal proteins is statistically significant, but also whether it is responsible for the bulk of observed translation inhibition.

To investigate whether the RuLX complexes inhibit efficient translation by binding to available, full-length DHFR, DHFR enzyme purchased form Sigma- Aldrich was treated with RuLX complexes at the highest exposure (80 µM) and its activity was measured using a DHFR assay (Figure 23B). The resultant data follows that RuL1-treated DHFR has similar activity to untreated DHFR. RuL2 and RuL3 appear to reduce the activity of DHFR due to their interactions with the enzyme. RuL2-treated DHFR has 20% less activity; it is possible that this small reduction activity may be insignificant when compared to untreated DHFR. More statistically robust experiments are needed to ensure this. Moreover, RuL3-treated DHFR consumes NADPH at half the rates that untreated DHFR does (Figure 23B). Such a significant reduction in activity could be indicative of such a vigorous interaction with the RuL3 complex that it degrades the DHFR enzyme. However, due to minimal materials and lack of time, only an exploratory investigation of these effects was conducted. A more robust investigation of the complexes is needed to delineate whether the contribution of RuLX interactions with active DHFR is statistically significant and whether it is responsible for the bulk of the inhibition of translation.

3.6. Follow-up studies investigating the impact and mechanism of RNA-RuL2 interactions in *in vitro* translation

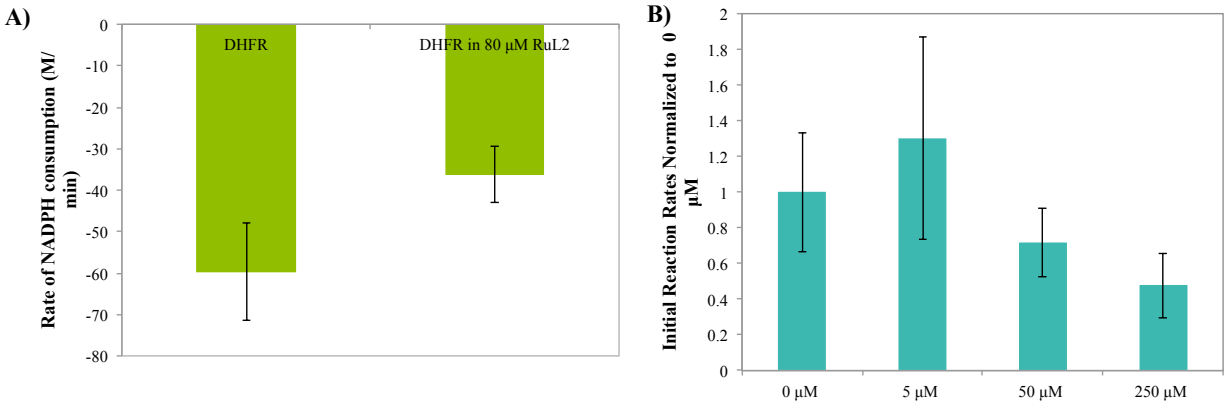

Figure 24: RuL2 dependent translation inhibition. **A)** Rate of consumption NADPH of DHFR compared to DHFR incubated with 80 μM RuL2. *t-test p>0.05* **B)** Normalized reaction rates (to those of 0 μM incubation) of *in vitro* translation product obtained with RuL2-treated RNA. *ANOVA p>0.05*

Due to the lack of significant agarose gel mobility changes in RuL1-treated RNA and the significant reduction of activity when the RuL3-treated DHFR enzyme, RuL1 and RuL3 complexes were not investigated for further triplicate studies. RuL2, due to its prevalent mobility shift in EMSA and seemingly minimal interaction with free DHFR enzyme, was selected for further analysis.

To follow-up on RuL2's ability to inhibit translation, triplicate translation events with RuL2-incubated RNA were carried out and their translation product measured for DHFR activity. While a dose-dependent trend is observed with regards to the reduction in DHFR activity, statistical analysis does not find them to be different from the activity of DHFR produced from untreated RNA or from each other [ANOVA p=0.321] (Figure 24B). Moreover, a control to rule out interactions between RuL2 and full-length DHFR as the source for the bulk of the inhibition was also conducted. Its results show that although there is a reduction in activity due to RuL2 interactions with the enzyme, the reduction appears statistically insignificant [t-test p= 0.287] (Figure 24B). In other words, the activity of untreated DHFR is essentially the same as the activity of RuL2-treated DHFR. Nevertheless, a more robust analysis of the inhibitory effects is needed due to the variability of the translation environment. An increase in replicates, from 3 to >5, could give data that is more insightful under statistical analysis. Moreover, outliers can more easily be singled out when a larger sample size is available. While RuL2 shows a dose-dependent reduction in enzyme activity when incubated with its DHFR mRNA, it is unlikely due to RuL2 impairing the activity of fully translated DHFR. However, it could be due to RuL2

impairment of the ribosomal proteins. This may account for some of the reduction in DHFR activity. However, due to minimal materials and lack of time, only an exploratory investigation of these effects was conducted. The data gathered so far, suggest that RuL2-dependet translation inhibition may be due to its interaction with the mRNA.

4. DISCUSSION

The explorative results obtained suggest that the RuLX complexes interact with both nucleic acids and proteins. They also show that treating RNA with the RuLX can inhibit mRNA directed *in vitro* translation. The data also suggest that the manner by which translation is inhibited, is different for each RuLX compound. Although the mechanism responsible for the bulk of the inhibition for each compounds is still unclear, more robust and specific experiments can be conducted in the future to reveal this relationship.

These *in vitro* studies show promising results where these complexes show chemical interactions with RNA and proteins. This allows for multiple avenues for inducing apoptosis when entered into cells. Moreover, the unique reactivity of the ruthenium and iron metal centers provides all three complexes with the potential to be selective against cancerous cells. Ruthenium (III) requires activation by reduction that is more likely in the acidic microenvironment of the tumor cells. Likewise, the ferroccene moiety can interconvert between its inert state and its active ferrocenium form depending on the redox potential of the tumor microenvironment. To support these findings, *in vivo* analyses of these complexes should be carried out in human cancerous cultures or tractable cancer model systems like *Saccharomyces cerevisiae*. An investigation of their antiproliferative properties as well as an analysis on their accumulation within the cell is needed.

4.1 Study design limitations

It is important to note the limitations of the current study design, which uses the reduction of enzyme activity as a measure of translation inhibition. This design does not reveal what aspect of translation is affected or impaired by the RuLX complexes. Whether incubation with RuLX

complexes inhibits translation initiation, which would result in no protein production, or cause early termination of translation, which would give truncated, inactive DHFR enzyme, cannot be determined using the current study design. Either of the aforementioned translation inhibition events would result in identical reduction of enzyme activity.

To remedy this, experiments investigating the inhibition of peptide synthesis using either ^{35}S labeled methionine or fluorescently labeled lysine should be conducted. Both labels are easily visualized using sodium dodecyl sulfate polyacrylamide gel electrophoresis (SDS-PAGE). The canonical sequence of DHFR possesses seven methionine residues and nineteen lysine residues suggesting that both labeling techniques would yield observable amplification of signal[49]. Moreover, the labeling can held delineate what aspect of translation is inhibited. If the RuLX complexes interfere with translation initiation, then there would be no successful peptide synthesis and thus no detection of peptides when examined using SDS-PAGE. On the other hand, if the interactions between the RuLX complexes and RNA cause a termination of translation, peptide chains smaller than 21 kDa (the molecular weight of the DHFR enzyme) would be observed using SDS-PAGE analysis. In the event that any of the RuLX complexes cause termination, peptide-sequencing studies should be carried out uncover the amino acid residues where termination frequently occurs. This could reveal more details of the downstream consequences of RNA and RuLX interactions.

4.2. RuL1

RuL1 possessed little to no interaction with RNA when examined by agarose gel electrophoresis. It is likely that the interaction between RuL1 and RNA, if any, is non-covalent. It would then be unlikely for this complex to inhibit translation by forming chemical interactions

with the RNA. It is important to note though, that the complex displayed translation inhibition in concentrations greater than 250 μM. The mechanism of this inhibition is unlikely to be through RNA-RuL1 interactions. However, it may be due to the complex's protein-RuL1 interactions. When investigated with DHFR enzyme and the translation machinery, RuL1 could impair the activity of both enzymes suggesting that its molecular target may be proteins rather than nucleic acids. *In vivo* studies investigating the binding affinity RuL1 to protein complexes are needed to ascertain the aforementioned hypothesis.

4.3. RuL2

RuL2 seems to be the most promising of the complexes as it not only possesses an interaction with RNA visible through an agarose EMSA, but also because it inhibits translation at a lower concentration than its counterpart RuL1. RuL2 inhibits translation at similar concentrations to RuL3. ICP-MS or MALDI-TOF analysis on the nature of the RNA-RuL2 interactions is needed to determine whether they are covalent. Also, such studies may provide evidence as to whether its imidazole moiety contributes to its reactivity with RNA, as NAMI-A's imidazole moiety does. Nevertheless, the strength RNA-RuL2 interactions may cause cytotoxicity in an *in vivo* model. Moreover, RuL2 appears to be able to weaken both DHFR and ribosomal protein activity, thus providing more evidence that RuL2 is capable of binding proteins. It could be the synergistic effects of both bonding to RNA and to proteins that allow this complex to inhibit translation at a concentration of 50μM.

4.4. RuL3

RuL3 appears to be the most potent of the three complexes. Not only does it have a more pronounced mobility shift when investigating its interactions with RNA, but it also shows a

considerable ability to hinder both DHFR activity and efficient translation by the ribosomal proteins when in incubated with them. Its interaction with RNA may allow for increased cytotoxicity (compared to RuL1 and RuL2) in an *in vivo* model. Moreover, its ability to significantly handicap protein activity is congruent with the EMSA evidence that suggested that RuL2 might be able to degrade proteins (Figure.8). *In vivo* analyses could further elaborate on RuL3's antiproliferative potential.

4.5. Future Experiments

Inductively coupled plasma mass spectrometry and matrix-assisted laser desorption/ionization time-of-flight (MALDI-TOF) mass spectrometry experiments should be conducted to reveal the nature of the RNA-RuLX interactions. Moreover, studies investigating the RuLX complexes binding affinity to DNA and RNA in the presence and absence of the reductant ascorbate should be carried out to investigate the activation by reduction hypothesis. These interactions should be characterized by both gel analysis and MALDI-TOF experiments. Hostetter and colleagues found that Ru-nucleotide interactions, in the context of NAMI-A and oligonucleotide biding, increase significantly in the presence of ascorbate. Furthermore, studies to determine whether ascorbate discourages the interconversion between ferroccene and ferrocenium salts of the RuLX complexes should also be conducted[47]. This is because, while ruthenium (II) is reduced to its active form ruthenium (II), ferroccene, wielding Fe (II), needs to be oxidized to its ferrocenium salt derivative, Fe (III), to possess antineoplastic and anti proliferative properties[27, 47].

To determine whether the inhibitory effects of RuLX are broad-range or specific to the DHFR mRNA, equivalent translation inhibition studies using β-galactosidase, luciferase or green

fluorescent protein mRNA as a new model should be conducted. All three aforementioned enzymes have established activities that are easily detected by their respective enzyme activity assays.

4.6. Concluding Remarks

It is evident from our studies that all three complexes possess the potential to inhibit translation. However, due to the differing strength of interactions with RNA, it is likely that these complexes inhibit translation through different mechanisms. More statistically robust studies could reveal whether these complexes inhibit translation primarily by binding to RNA or by denaturing proteins. An investigation on the antiproliferative and antineoplastic potential of the RuLX complexes should be conducted in tractable cancer model systems like *Saccharomyces cerevisiae.* Nevertheless, these complexes possess great potential to inhibit translation and become a possible addition into the arsenal of metal-centered chemotherapeutic complexes.

References

(1) The International Agency for Research on Cancer. "Globocan." Fact Sheets by Population. World Health Organization, 2012. (Accessed Nov 06 , 2014)

(2) Hanahan, D.; Weinberg, R. A. The Hallmarks of Cancer. *Cell* **2000**, *100* (1), 57–70.

(3) Pellegrino, Teresa; Parak, Wolfgang J.; Boudreau, Rosanne; Le gros, Mark A.; Gerion, Daniele; Alivisatos, A. Paul, Larabell, Carolyn A. Quantum dot-based cell motility assay. *Differentiation*. **2003**. *71, 542-548.*

(4) Hanahan, D.; Weinberg, R. a. Hallmarks of Cancer: The next Generation. *Cell* **2011**, *144* (5), 646–674.

(5) Sherr, C. J. Principles of Tumor Suppression Review. **2004**, *116*, 235–246.

(6) American Cancer Society. "Treatment Types". Types of Cancer Treatment. American Cancer Society, 2014. (Accessed October 29, 2014). http://www.cancer.org/treatment/treatmentsandsideeffects/treatmenttypes/treatment-types-landing

(7) Alderden, R. A.; Hall, M. D.; Hambley, T. W. Products of Chemistry The Discovery and Development of Cisplatin. **2006**, *83* (5).

(8) Rosenberg, B.; Vancamp, L.; Trosko, J.E.; Mansour, V. Platinum Compounds: a New Class of Potent Antitumor Agents. *Nature*. **1969**, *222, 385-386.*

(9) Prestayko, Archie W.; Stanley T. Crooke; and Stephen K. Carter. *Cisplatin, Current Status and New Developments*. New York: Academic, 1980.

(10) Jamieson, E. R.; Lippard, S. J. Structure, Recognition, and Processing of Cisplatin−DNA Adducts. *Chem. Rev.* **1999**, *99* (9), 2467–2498.

(11) Gasser, G.; Ott, I.; Metzler-Nolte, N. Organometallic Anticancer Compounds. *J. Med. Chem.* **2011**, *54*, 3–25.

(12) Wang, D.; Lippard, S. J. Cellular Processing of Platinum Anticancer Drugs. *Nat. Rev. Drug Discov.* **2005**.

(13) Pizzaro, A.M.; Habtemariam, A.; Sadler, P.J. Activation Mechanisms for Organometallic Anticancer Complexes. *Top Organomet. Chem*. **2010**. *32, 21–56.* (14)

(14) Wheate, N. Multi-Nuclear Platinum Complexes as Anti-Cancer Drugs. *Coord. Chem. Rev.* **2003**, *241* (1-2), 133–145.

(15) Suo, Z.; Lippard, S. J.; Johnson, K. A. Single D (GpG)/ Cis -Diammineplatinum (II) Adduct-Induced Inhibition of DNA Polymerization. **1999**, No. Ii, 715–726.

(16) Rosenberg, J., & Sato, P. Messenger RNA loses the ability to direct in vitro peptide synthesis following incubation with cisplatin. *Mol. Pharmacol.* **1988**. *33* (6), 611-616.

(17) Rosenberg, J. M., & Sato, P. H. Cisplatin inhibits in vitro translation by preventing the formation of complete initiation complex. *Mol. Pharmacol.* **1993**. *43(3), 491-497*

(18) Siddik, Z. H. Cisplatin: Mode of Cytotoxic Action and Molecular Basis of Resistance. *Oncogene* **2003**.

(19) Brabec, V.; Novakova, O. DNA Binding Mode of Ruthenium Complexes and Relationship to Tumor Cell Toxicity. *Drug Resist. Updat.* **2006**, *9* (3), 111–122.

(20) Hannon, M. J. Metal-Based Anticancer Drugs: From a Past Anchored in Platinum Chemistry to a Post-Genomic Future of Diverse Chemistry and Biology. *Pure and Applied Chemistry*, 2007.

(21) Clarke, M. J. Ruthenium Metallopharmaceuticals. *Coord. Chem. Rev.* **2002**, *232* (1-2), 69–93.

(22) Wang, D.; Lippard, S. J. Cellular Processing of Platinum Anticancer Drugs. *Nat. Rev. Drug Discov.* **2005**.

(23) Clarke, M. J.; Zhu, F.; Frasca, D. R. Non-Platinum Chemotherapeutic Metallopharmaceuticals. *Chem. Rev. (Washington, D. C.)* **1999**, *99*, 2511–2533.

(24) Pluim, D.; Van Waardenburg, R. C. a M.; Beijnen, J. H.; Schellens, J. H. M. Cytotoxicity of the Organic Ruthenium Anticancer Drug Nami-A Is Correlated with DNA Binding in Four Different Human Tumor Cell Lines. *Cancer Chemother. Pharmacol.* **2004**, *54* (1), 71–78.

(25) Bacac, M.; Hotze, A. C. .; Schilden, K. van der; Haasnoot, J. G.; Pacor, S.; Alessio, E.; Sava, G.; Reedijk, J. The Hydrolysis of the Anti-Cancer Ruthenium Complex NAMI-A Affects Its DNA Binding and Antimetastatic Activity: An NMR Evaluation. *J. Inorg. Biochem.* **2004**, *98* (2), 402–412.

(26) Sava, G.; Capozzi, I.; Clerici, K.; Gagliardi, G.; Alessio, E.; Messtroni, G. Pharmacological control of lung metastases of solid tumors by a novel ruthenium complex. *Clin Exp Metastasis*. **1998**. *16, 371–379*

(27) Kopf-Maier, P., Kopf, H., & Neuse, E. W. Ferrocenium salts—the first antitumor iron compounds. *Angewandte Chemie*. **1984**. *96 (6), 446-447.*

(28) Osella, D.; Ferrali, M.; Zanello, P.; Laschi, F.; Fontani, M.; Nervi, C.; Cavigiolio, G. On the Mechanism of the Antitumor Activity of Ferrocenium Derivatives. *Inorganica Chim. Acta* **2000**, *306* (1), 42–48.

(29) Prussin, A. J.; Zhao, S.; Jain, A.; Winkel, B. S. J.; Brewer, K. J. DNA Interaction Studies of Tridentate Bridged Ru(II)-Pt(II) Mixed-Metal Supramolecules. *J. Inorg. Biochem.* **2009**, *103* (3), 427–431.

(30) Milkevitch, M.; Shirley, B. W.; Brewer, K. J. Mixed-Metal Polymetallic Platinum Complexes Designed to Interact with DNA. *Inorganica Chim. Acta* **1997**, *264* (1-2), 249–256.

(31) Miao, R.; Mongelli, M. T.; Ziegler, D. F.; Winkel, s. S.; Brewer, K. J. A Multifunctional Tetrametallic Ru-Pt Supramolecular Complex Exhibiting Bith DNA Binding and Photocleavage. *Inorganic Chem.* **2006**, *45* (126), 10413–10415.

(32) Anderson, C. M.; Taylor, I. R.; Tibbetts, M. F.; Philpott, J.; Hu, Y.; Tanski, J. M. Hetero-Multinuclear ruthenium(III)/platinum(II) Complexes That Potentially Exhibit Both Antimetastatic and Antineoplastic Properties. *Inorg. Chem.* **2012**, *51* (23), 12917–12924.

(33) Herman, A.; Tanski, J. M.; Tibbetts, M. F.; Anderson, C. M. Synthesis, Characterization, and in Vitro Evaluation of a Potentially Selective Anticancer, Mixed-Metal [ruthenium(III)-platinum(II)] Trinuclear Complex. *Inorg. Chem.* **2008**, *47* (1), 274–280.

(34) Jain, S. S.; Anderson, C. M.; DiRienzo, F.; Taylor, I. R.; Jain, K.; Guha, S.; Hoque, N. RNA Binding and Inhibition of Primer Extension by a Ru(iii)/Pt(ii) Metal Complex. *Chem. Commun.* **2013**, *49* (44), 5031–5033.

(35) Anderson, C. M.; Jain, S. S.; Silber, L.; Chen, K.; Guha, S.; Zhang, W.; McLaughlin, E. C.; Hu, Y.; Tanski, J. M. Synthesis and Characterization of Water-Soluble, Heteronuclear ruthenium(III)/ferrocene Complexes and Their Interactions with Biomolecules. *J. Inorg. Biochem.* **2015**, *145*, 41–50.

(36) Kissai, M., Anderson, C. M., Jain, S. Investigating the Binding Potential of Hetero-multinuclear Organometallic Complexes to Albumin from Bovine Serum. Presented at the Bard Summer Research Institute Poster Session, Annandale-on-Hudson, NY, United States, September 23, 2014

(37) Nelson, David L., Michael M. Cox, and Albert L. Lehninger. *Lehninger Principles of Biochemistry*, 6th ed. New York: W.H. Freeman, 2013; pp 1051-067.

(38) Graff, J. R.; Konicek, B. W.; Carter, J. H.; Marcusson, E. G. Targeting the Eukaryotic Translation Initiation Factor 4E for Cancer Therapy. Cancer Res. 2008, 68 (3), 631–634.

(39) Bordeleau, M.; Robert, F. Therapeutic Suppression of Translation Initiation Modulates Chemosensitivity in a Mouse Lymphoma Model. *J. Clin. Invest.* **2008**, *118* (7), 1–10.

(40) Cencic, R.; Carrier, M.; Galicia-Vázquez, G.; Bordeleau, M.-E.; Sukarieh, R.; Bourdeau, A.; Brem, B.; Teodoro, J. G.; Greger, H.; Tremblay, M. L.; et al. Antitumor Activity and Mechanism of Action of the Cyclopenta[b]benzofuran, Silvestrol. *PLoS One* **2009**, *4* (4), e5223.

(41) Gready, J. E., Dihydrofolate reductase: binding of substrates and inhibitors and catalytic mechanism. *Adv*. *Pharmacol*. *Chemother*. **1980**, *17, 37-102*.

(42) Blakley, R. L., Eukaryotic dihydrofolate reductase. *Adv*. *Enzymol*. *Relat*. *Areas Mol*. *Biol*. **1995**, *70, 23-102*.

(43) Costi, M. P., and Ferrari, S., Update on antifolate drugs targets. *Curr*. *Drug Targets*. **2001**, *2, 135-166*.

(44) *QIAGEN® Plasmid Purification Handbook 3rd ed.* (2005). QIAGEN, Nov. 2005. (accessed September 2014). <https://www.qiagen.com/us/resources/resourcedetail?id=fc49b220-129b-4b0f-bab0-3de3e89c1525&lang=en>.

(45) Corp., Sigma-Aldrich. *Dihydrofolate Reductase Assay Kit Technical Bulletin*. Dihydrofolate Reductase Assay Kit (CS0340) – Bulletin.

(46) Iwamoto, T.; Hiraku, Y.; Oikawa, S.; Mizutani, H.; Kojima, M.; Kawanishi, S. DNA Intrastrand Cross-Link at the 5′-GA-3′ Sequence Formed by Busulfan and Its Role in the Cytotoxic Effect. *Cancer Sci.* **2004**, *95* (5), 454–458.

(47) Hostetter, A. a; Osborn, M. F.; DeRose, V. J. Characterization of RNA-Pt Adducts Formed from Cisplatin Treatment of Saccharomyces Cerevisiae. *ACS Chem Biol.* **2012**, *7* (1), 218–225.

(48) Burmann, B. M.; Schweimer, K.; Luo, X.; Wahl, M. C.; Stitt, B. L.; Gottesman, M. E.; Rösch, P. A NusE:NusG Complex Links Transcription and Translation. *Science* **2010**, *328* (5977), 501–504.

(49) The UniProt Consortium. The Universal Protein Resource (UniProt). *Nucleic Acids Research*. **2008** ; 36(Database issue):D190-D195. doi:10.1093/nar/gkm895.

Vita

Mildred Apollo Kissai was born in Dar es Salaam, Tanzania. After completing most of her primary school education in Diamond Primary School in Upanga, Dar es Salaam, she relocated with her parents to Doha, Qatar where she attended the American School of Doha (ASD). She received her high school diploma from ASD in June 2011 and enrolled at Bard College in Annandale-on-Hudson, NY. She is excited to receive her Bachelor of Arts with a major in Biology and Chemistry from Bard College in May 2015.